Systematische Identifizierung von Krankheitsgenen für intestinale und urogenitale Fehlbildungen mittels „Whole Exome Sequencing“ (WES)

Inaugural-Dissertation

zur Erlangung des Doktorgrades

der Hohen Medizinischen Fakultät

der Rheinischen Friedrich-Wilhelms-Universität

Bonn

Franziska Kause-Zriouil, geb. Kause

aus Lüneburg

2021

Angefertigt mit der Genehmigung
der Medizinischen Fakultät der Universität Bonn

1. Gutachter*in: Prof. Dr. med. Heiko M. Reutter
2. Gutachter*in: PD Dr. Alfredo Estanislao Ramirez Zuniga

Tag der Mündlichen Prüfung: 10.05.2021

Aus dem Institut für Humangenetik
Direktor: Prof. Dr. med. Markus M. Nöthen

Inhaltsverzeichnis

	Abkürzungsverzeichnis	5
1.	**Deutsche Zusammenfassung**	6
1.1	Einleitung	6
1.2	Material und Methoden	8
1.3	Ergebnisse	10
1.4	Diskussion	14
1.5	Zusammenfassung	16
1.6	Literaturverzeichnis der deutschen Zusammenfassung	17
2.	**Publikation A: *HSPA6*: A new autosomal recessive candidate gene for the VATER/VACTERL malformation spectrum**	
	Abstract	22
	Introduction	23
	Materials and Methods	23
	Results	24
	Discussion	26
	References	27
3.	**Publikation B: Whole exome sequencing identifies a mutation in *EYA1* and *GLI3* in a patient with branchiootic syndrome and esophageal atresia: coincidence or a digenic mode of inheritance?**	
	Abstract	29
	Introduction	29
	Materials and Methods	30
	Results	30
	Discussion	32
	References	33
4.	**Publikation C: CAKUT and autonomic dysfunction caused by acetylcholine receptor mutations**	
	Abstract	35
	Report	35
	References	41

5. Danksagung 43

Abkürzungsverzeichnis

ARM	Anorektale Malformation(en)
Abb.	Abbildung
BO-Syndrom	Branchio-otisches Syndrom
BOR-Syndrom	Branchio-oto-renales Syndrom
CAKUT	congenital anomalies of the kidney and urinary tract (kongenitale Anomalien der Nieren und ableitenden Harnwege)
cDNA	complementary deoxyribonucleic acid (komplementäre Desoxyribonukleinsäure)
CNV	copy number variation (Kopienzahl-Veränderung)
DNA	Desoxyribonukleinsäure
EA/TEF	esophageal atresia/tracheoesophageal fistula (Öophagusatresie/Tracheoösophageale Fistel)
LUTO	lower urinary tract obstruction (Verengung der unteren ableitenden Harnwege)
qPCR	quantitative polymerase chain reaction (quantitative Polymerase-Kettenreaktion)
VACTERL	Vertebral defects (Wirbelkörperfehlbildungen) Anorectal malformations (anorektale Fehlbildungen) Cardiac defects (kardiale Fehlbildungen) Tracheoesophageal fistula (tracheo-ösophageale Fistel) Esophageal atresia (Ösophagusatresie) Renal malformations (renale Fehlbildungen) Limb defects (Extremitätenfehlbildungen)
WES	whole exome sequencing (Exom-Sequenzierung)

1. Deutsche Zusammenfassung

1.1 Einleitung

Anorektale Malformationen (ARM) und Ösophagusatresien, mit oder ohne tracheoösophagealer Fistel (EA/TEF), sind seltene Fehlbildungen des embryonalen Vorder- und Hinterdarms. Sie kommen mit einer Prävalenz von 1 pro 3.000-4.000 Lebendgeburten vor (Cuschieri, 2001; Depaepe et al., 1993). Ein gemeinsames Auftreten mit anderen Fehlbildungen ist in 50-60% der Fälle zu beobachten (De Jong et al., 2010; Cuschieri et al., 2001; Balanescu et al., 2013). Hierbei ist am häufigsten zusätzlich der Urogenitaltrakt mit etwa 80% betroffen (Stoll et al., 2007). Eine alleinige Kombination von ARM und Fehlbildungen der oberen Gliedmaßen tritt in etwa 6% der Fälle auf (van den Hondel et al., 2016). ARM und EA/TEF treten ebenfalls als Teil von genetischen Syndromen und Assoziationen auf, z.B. im Rahmen der VATER/VACTERL-Assoziation. Diese beschreibt das gleichzeitige Auftreten von mindestens drei Fehlbildungen in folgenden Organsystemen: Wirbelsäule (V), anorektale Malformation (A), kardiale Defekte (C), tracheoösophageale Fistel mit oder ohne Ösophagusatresie (TE), renale Fehlbildungen (R), Fehlbildungen der Extremitäten (L). Liegen nur in zwei dieser Organsysteme Fehlbildungen vor, wird dieses als VATER/VACTERL-ähnliche Assoziation bezeichnet. Über die genetischen Ursachen von ARM und EA/TEF ist bisher wenig bekannt. Saisawat et al. konnten ein rezessives Krankheitsgen, *TRAP1*, in Zusammenhang mit ARM bzw. der VATER/VACTERL-Assoziation und kongenitalen Anomalien der Nieren und der abführenden Harnwege (congenital anomalies of the kidney and urinary tract, CAKUT) beschreiben (Saisawat et a., 2014). In Mausmodellen wurden *Gli2* und *Gli3* als essenziell für die embryologische Entwicklung der Speiseröhre identifiziert (Motoyoma et al, 1998). Beide sind Teil des Hedgehog-Signalwegs.

CAKUT sind der häufigste Grund für eine chronische Niereninsuffizienz in den ersten drei Lebensdekaden und treten mit einer Prävalenz von 3-6 pro 1.000 Lebendgeburten auf. Eine Verengung der unteren ableitenden Harnwege (Lower Urinary Tract Obstruction, LUTO) ist hierbei durch sekundäre Folgen eines Harnaufstaus, wie zum Beispiel bei vesikoureteralem Reflux (VUR) oder Hydronephrose, eine wichtige Ursache für die chronische Niereninsuffizienz. Monoallelische und biallelische Varianten in über 40 Genen sind als verursachend für CAKUT identifiziert worden, können jedoch nur bei ca.

5%-20% der Patienten die Fehlbildungen erklären (van der Ven et al., 2018). Vorherrschend sind hierbei Gene, die in die Regulation wichtiger embryologischer Entwicklungsprozesse des Urogenitaltraktes eingebunden sind (van der Ven et al., 2018; Vivante et al., 2014). Zu beachten sind jedoch auch Gene, die verantwortlich für die neuronale Regulation der Blasenentleerung sind. Bisher wurden in diesem Zusammenhang biallelische Varianten in dem Gen *CHRM3* gefunden, welche zu einer Verengung der unteren ableitenden Harnwege führen (Weber et al., 2011).

Das Ziel der drei Studien zu ARM, EA/TEF und CAKUT war, Kandidatengene mittels „whole exome sequencing“ (WES) zu identifizieren und zu re-sequenzieren.

In **Publikation A** lag der Schwerpunkt auf der Suche nach autosomal-rezessiven (biallelischen) und X-chromosomal-rezessiven Kandidatengenen in drei Familien mit ARM oder VATER/VACTERL-ähnlichem Phänotyp.

Publikation B beschreibt einen Indexpatienten, bei dem eine EA/TEF mit dem seltenen autosomal-dominant vererbten branchio-otischen Syndrom (BOS1: OMIM #602588) zusammenfällt. Dieses hat eine Geburtenprävalenz von 1 pro 40.000 Lebendgeburten (Fraser et al., 1980) und ist gekennzeichnet durch Fehlbildungen der embryonalen Kiemenbogen und der Ohren. Das BO-Syndrom ist allelisch zum branchio-oto-renalen Syndrom (BOR1: OMIM #113650) (Vincent et al., 1997), bei welchem zusätzlich Fehlbildungen der Nieren auftreten. Ursächlich für beide Krankheitsbilder, BOS1 und BOR1, sind monoallelische Varianten in *EYA1* und *SIX1* (Abdelhak et al., 1997, Vincent et al., 1997; Ruf et al., 2003; Ruf et al., 2004). Für das BOR-Syndrom sind zusätzlich ursächliche Varianten in *SIX5* (Hoskins et al., 2006) bekannt. Hier sollte ein möglicher Zusammenhang zwischen der EA/TEF und dem BO-Syndrom im Indexpatienten genetisch untersucht werden.

Ziel der in **Publikation C** besprochenen Studie war ebenfalls, autosomal-rezessive (biallelische) Kandidatengene bei einem Patienten mit CAKUT und neurogener Blasenstörung zu identifizieren. Für diese Studie führte die Arbeitsgruppe von Prof. Dr. Friedhelm Hildebrandt am Boston Children’s Hospital, Department of Pediatrics/Boston

(USA) ein „Homozygosity mapping“ (Homozygotie-Kartierung) durch (Hildebrandt et al., 2009). Die aus dem „Homozygosity mapping“ generierten Daten wurden auf Anhäufung homozygoter Regionen im Genom hin untersucht. Die durch WES gewonnenen Sequenz-Daten filterte ich systematisch auf rezessive (biallelische) Varianten in diesen homozygoten Regionen. Zur funktionellen Untersuchung des Kandidatengens führte ich unter anderem zellbiologische Methoden an HEK293 Zellen durch (HEK=human embryonic kidney).

1.2 Material und Methoden

In den drei Studien kamen bei den Indexpatienten und -familien grundlegend molekulargenetische Methoden zum Einsatz: Für Publikation A und B bereitete ich die „DNA libraries“ der einzelnen Patienten vor. Die WES-Daten generierte dann unser Kooperationspartner Cologne Center for Genomics/Universität Köln mit einem IlluminaHiSeq2500 Sequencer. Ich wertete diese mit dem Exom- und Genom-Analyse-Programm „Varbank“ aus (https://varbank.ccg.uni-koeln.de). Für Publikation C wurden mittels einer Illumina™ Plattform WES-Daten generiert, die ich mit dem Exom-und-Genom-Analyse-Programm CLC Genomics Workbench (version 6.5.1) (CLC bio) auswertete. Der Schwerpunkt lag hier auf Regionen, die sich im „Homozygosity mapping“ als vererbt homozygot zeigten. Die Priorisierung der Varianten erfolgte mithilfe einer Begrenzung der Allelfrequenz auf <0.5% in der allgemeinen Bevölkerung, der Anwendung von Vorhersage-tools über Veränderung der Proteinfunktion und der -konformation, von Expressionsdaten aus online-Datenbanken und von Herausarbeitung der embryonalen Funktion und Expression sowie eingehender PubMed-Literaturrecherche (www.ncbi.nlm.nih.gov/pubmed). Validierung sowie Segregationsanalysen der identifizierten Varianten führte ich in allen Studien mit Sanger-Sequenzierung durch. Die Patienten in Publikation A und B wurden über das Netzwerk zu Kongenitalen Uro-Rektalen Fehlbildungen (CURE-Net, www.cure-net.de) und das „great-consortium“ (genetic risk of esophagel atresia, wwww.great-konsortium.de) rekrutiert. In allen drei Studien legten die Eltern der teilnehmenden Patienten vor Beginn der Untersuchungen unterschriebene Einverständniserklärungen vor. Die Ethikkomissionen der jeweiligen beteiligten Institutionen genehmigten die Patientenrekrutierung und Durchführung der genetischen Studien.

In **Publikation A** wurden drei Geschwisterpaare mit ARM oder VATER/VACTERL-ähnlichem Phänotyp und deren gesunde Eltern untersucht (Familie 1098, Familie 971, Familie 1346). In Familie 1346 zeigte das betroffene Geschwisterpaar einen VATER/VACTERL-ähnlichen Phänotyp mit ARM, Hypoplasie und Ankylose beider kleinen Finger bei der Schwester und isolierter Radiushypoplasie bei dem Bruder (Abb. 1). Mittels WES und Sanger-Sequenzierung suchte ich in den drei Familien nach rezessiven homozygoten, compound-heterozygoten und X-chromosomalen Varianten. Bei Familie 1346 wandte ich zusätzlich eine auf SYBR® Green basierte qPCR (quantitative polymerase chain reaction) zur Identifizierung von copy number variations (CNVs) an. Zur weiteren Untersuchung des in der Folge beschriebenen Kandidatengens re-sequenzierte ich dieses nach Sanger in 167 Patienten mit VATER/VACTERL- und VATER/VACTERL-ähnlicher Assoziation, die mit ARM und Fehlbildungen der Gliedmaßen einen ähnlichen Phänotyp wie die betroffenen Kinder dieser Familie hatten.

In **Publikation B** wies der Indexpatient eine EA/TEF vom Typ Vogt IIIb (Vogt, EC, 1929) und ein BO-Syndrom mit beidseitigen Hals- und Ohrfisteln auf. Seine Mutter und seine Schwester zeigten ebenfalls Merkmale des BO-Syndrom mit einseitigem Hörverlust und unilateraler Ohrfistel bei der Mutter und bilateralen Ohrfisteln sowie unilateraler Halsfistel bei der Schwester. Der Bruder wies lediglich ein unspezifisches präaurikuläres Grübchen auf (Abb.2). Initial untersuchte ich den Indexpatienten auf Varianten in *EYA1*, *SIX1* und in Genen, die mit beiden im Hedgehog-Signalweg interagieren. Für alle identifizierten Varianten führte ich dann eine Segregationsanalyse bei Geschwistern und Eltern durch. Zusätzlich untersuchte ich mit Sequenzierung nach Sanger 18 weitere Patienten mit EA/TEF und BO-Syndrom assoziierten Anomalien (Hörverlust oder Fehlbildungen der Ohren).

In **Publikation C** zeigte der Indexpatient eine neurogene Blasenstörung mit vesikoureteralem Reflux (VUR) Grad 5, Hydronephrose und progressiver Niereninsuffizienz. Zusätzlich fielen in der augenärztlichen Untersuchung weite und fixierte Pupillen, entsprechend einer Mydriasis, auf (Abb. 3). Entsprechend der familiären Vererbung der Fehlbildungen (gesunde Eltern und betroffenes Kind) filterte ich die WES-Daten nach rezessiven (biallelischen bzw. X-chromosomalen) Varianten. Über das online-

Netzwerk Genematcher (https://genematcher.org/statistics) und Screening einer hauseigenen Kohorte von 380 Familien mit CAKUT suchte ich nach weiteren Patienten mit rezessiven Varianten in dem durch WES identifizierten Krankheitsgen. Die über Genematcher einbezogenen Patienten wurden durch unsere Kooperationspartner an den Universitäten von Bristol (Vereinigtes Königreich) und Exeter (Vereinigtes Königreich) klinisch untersucht, die auch ihre Sequenzdaten generierten. Unser Kooperationspartner an der Yale Universität, Department of Genomics/New Haven (USA) generierte die WES-Daten des Indexpatienten und der hauseigenen Kohorte. Für die funktionelle Untersuchung der Mutationen führte ich Immunofluoreszenz-Experimente in HEK293 Zellen durch. In cDNA (complementary deoxyribonucleid acid) fügte ich hierfür die identifizierten Mutationen mittels zielgerichteter Mutagenese ein und brachte sie als C-terminale GFP-markierte Konstrukte in die HEK293 Zellen ein. Wildtyp- und mutierte Proteine lokalisierte ich mit konfokaler Fluoreszenzmikroskopie in den Zellen. Zusätzlich wurden durch unsere Kooperationspartner an der University of Texas, Southwestern Medical Center/Texas (USA) ektrophsyiologische Studien mit patch-clamp-Technik ebenfalls in HEK293 Zellen durchgeführt.

1.3 Ergebnisse

Publikation A: Die hier untersuchten Daten der drei Familien wurden auf rezessive homozygote, compound-heterozygote und X-chromosomale Varianten hin gefiltert. In Familie 1346 identifizierte ich bei dem betroffenen Geschwisterpaar eine zunächst scheinbar homozygote Variante in *HSPA6* (c.1340G>T, gemäß ENSEMBL GRCh37/hg19 Transkript ENST00000309758). Die Segregationsanalyse zeigte jedoch, dass nur die Mutter heterozygote Trägerin der Variante war und der Vater einen Wildtyp aufwies. Mittels qPCR konnte ich folgend nachweisen, dass der Vater eine Deletion von *HSPA6* trägt. Beide Kinder erbten diese Deletion vom Vater. Somit sind beide Kinder compound-heterozygot für die Deletion ihres Vaters und die Punktmutation ihrer Mutter (Abb. 1). Als Regulator von Zellzyklen und Teil apoptischer Signalkaskaden ist HSPA6 ein wichtiger protektiver Faktor während der embryonalen Entwicklung (Luft & Dix, 1999). Um weitere Familien mit Varianten in *HSPA6* zu identifizieren, sequenzierte ich 167 Patienten mit

ARM und VATER/VACTERL-ähnlichem Phänotyp. Dabei ließen sich keine weiteren biallelischen Varianten in *HSPA6* identifizieren.

In Familie 971 zeigten sich compound-heterozygote Varianten in *ITSN2* (c.1442T>A und c.4367A>G, entsprechend ENSEMBL GRCh37/hg19 Transkript ENST00000355123). Variante c.1442T>A (p.Ile481Asn) stufte ich mithilfe der Vorhersage-tools als schädigend ein. Variante c.4367A>G (single nucleotide polymorphism [SNP]: rs139986826; p.Asn1456Ser) erwies sich jedoch als benigne, da ein geringer Einfluss auf die Proteinfunktion und -konformation vorlag und die Aminosäure Alanin an dieser Stelle nur schwach konserviert ist. Hiermit konnten beide Varianten als Ursache der Fehlbildungen in einem compound-heterozygoten Erbgang ausgeschlossen werden.

In Familie 1098 wurden keine rezessiven Varianten identifiziert.

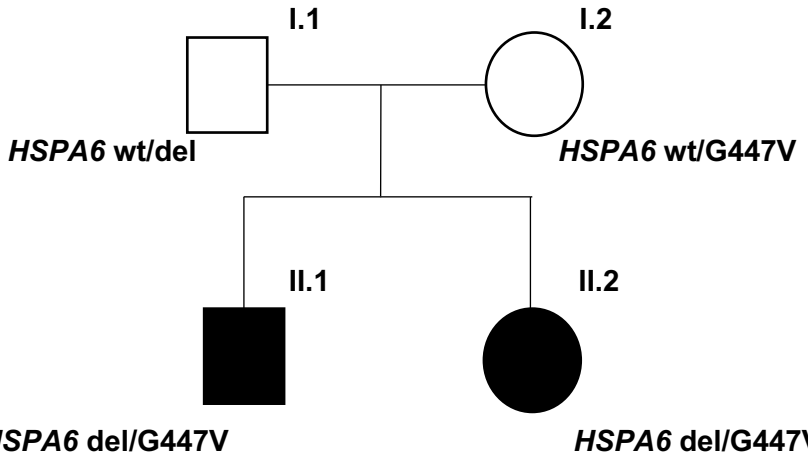

Abb. 1: Stammbaum der in Publikation A untersuchten Familie 1346.
1346_II.1: isolierte radiale Hypoplasie beidseits.
1346_II.2: anorektale Malformation in Form einer perinealen Fistel, Hypoplasie und Ankylose beider kleinen Finger.
Durch WES und qPCR identifizierte Mutationen und Wildtyp sind angezeigt. HSPA6, heat shock 70kD protein 6; wt, Wildtyp; del, Deletion; G, Glycin; V, Valin.

Publikation B: Meine WES-Analyse ergab bei dem Indexpatienten eine vorbeschriebene *EYA1*-Mutation in der Donor-Spleißstelle von Exon 10 (c.966+5G>A, entsprechend ENSEMBL Transkript ENST00000340726) (Stockley et al., 2009; Krug et al., 2011; Song et al., 2013; Berkheineria et al., 2017). Diese konnte ebenfalls bei den vom BO-Syndrom betroffenen Familienmitgliedern, Schwester und Mutter des Indexpatienten, identifiziert

werden. Das weitere Filtern der WES-Daten zeigte in den mit *EYA1* und *SIX1* interagierenden Genen folgende Varianten: *GLI1* (p.Thr176Met), *GLI3* (Spleiß-Variante c.1028+3A>G, rs368499795, entsprechend ENSEMBL Transkript ENST00000395025), *NRP1* (p.Asp601Asn) und *SMO* (p.Arg168His) (Abb. 2). Von den Varianten in *GLI1*, *GLI3*, *NRP1* und *SMO* berücksichtigte ich in der Folge nur die Varianten, die der gesunde Vater ausschließlich auf den Indexpatienten übertrug, da hier möglicherweise durch das Zusammenspiel mit der *EYA1*-Mutation im Sonic-hedgehog pathway das Auftreten von BO-Syndrom und EA/TEF im Indexpatienten verursacht wurde. Alleine die heterozygote *GLI3* Spleiß-Variante c.1028+3A>G erfüllte dieses Kriterium. Laut „Human Splicing Finder 3.0“ (Desmet et al., 2009) sowie nach Shapiro und Senapathy (Shapiro und Senapathy, 1987) kann diese den korrekten Spleiß-Vorgang behindern. Die Varianten in *GLI1*, *NRP1* und *SMO* wurden ausgeschlossen, da diese entweder von der Mutter, welche keine EA/TEF aufwies, an die Kinder vererbt wurden oder, im Fall der *NRP1*- und *SMO*-Variante, gering konserviert bzw. zu häufig waren. Das Screening einer Kohorte von 18 Patienten mit EA/TEF und Merkmalen des BO-Syndroms konnte keine weiteren potentiell krankheitsverursachenden Varianten in *EYA1* aufdecken.

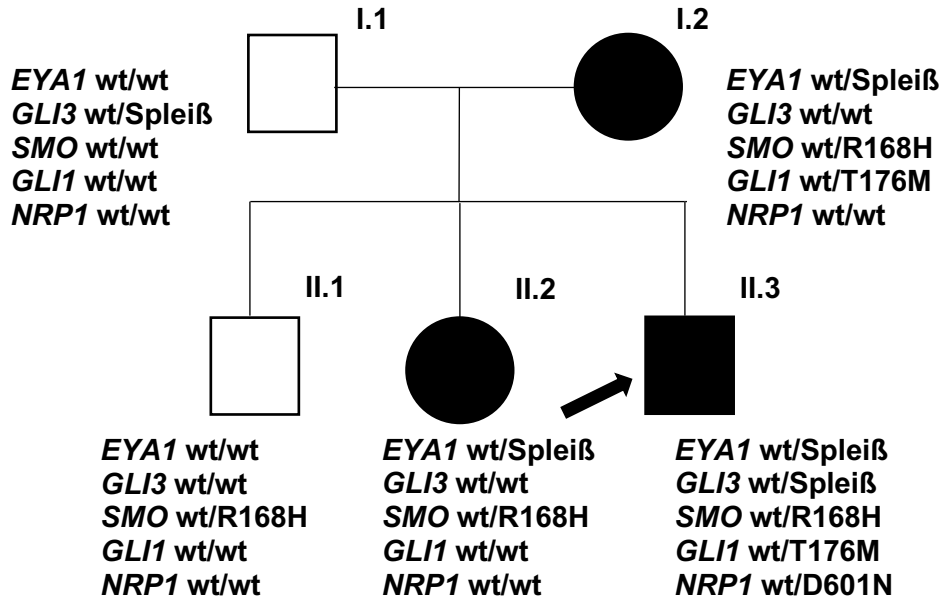

Abb. 2: Stammbaum der in Publikation B untersuchten Familie.
I.2: BO-Syndrom (einseitiger Hörverlust, unilaterale Ohrfistel)
II.2: BO-Syndrom (bilaterale Ohrfisteln, unilaterale Halsfistel)

II.3: Öophagusatresie/Tracheoösophageale Fistel Typ Vogt IIIb, BO-Syndrom (beidseitige Hals- und Ohrfisteln).
Der Indexpatient wird durch einen Pfeil markiert. Durch WES und Sanger Sequenzierung identifizierte Mutationen und Wildtyp sind angezeigt. BO-Syndrom, Branchio-otisches Syndrom; wt, Wildtyp; Spleiß, Spleiß-Variante; EYA1, Drosophila eyes absent; GLI, GLI family zinc finger; SMO, smoothened, frizzled class receptor; NRP1, neuropilin 1; R, Arginin; H, Histidin; T, Threonin; D, Asparaginsäure; M, Methionin; N, Asparagin.

Publikation C: Bei dem Indexpatienten und seinem betroffenen Bruder identifizierte ich rezessiv-homozygote Varianten in *CHRNA3* (entsprechend ENSEMBL Transkript ENST00000326828.5; c.1010_1011delCA, p.T337Nfs*81) (Abb. 3). *CHRNA3* kodiert die α-Untereinheit des $\alpha_3\beta_4$-nikotinischen Rezeptors ($\alpha_3\beta_4$-nAchR). Über Genematcher fand sich dann ein betroffenes Geschwisterpaar von konsanguinen Eltern, welches eine homozygote Variante aufwies (c.1019C>G, p.S340*). Beide Varianten, p.T337Nfs*81 und p.Ser340*, sind potentiell trunkierend und können möglicherweise zu einer Verkürzung des Proteins vor der vierten Transmembranhelix führen. Nach Screening von 666 WES-Datensätzen (380 Familien) der eigenen CAKUT-Kohorte konnte eine Spleiß-Variante in einer Patientin identifiziert werden (c.267+2T>G), welche vermutlich zum Aussetzen von Exon 3 und einer in-frame Deletion von 15 Aminosäuren in der extrazellulären Ligandenbindungsstelle führt. Alle drei genannten Patienten wiesen einen ähnlichen urogenitalen und ophtalmologischen Phänotyp auf wie der Indexpatient. CHRNA3 ist ein Membranprotein, welches als Teil des α3β4-nAchR fungiert. In den Lokalisationsstudien in HEK293 Zellen zeigte sich, dass nur der Wildtyp vollständig an der Zellmembran vorhanden war. Die den Mutationen p.T337Nfs*81 und p.S340* entsprechenden trunkierten Proteinen wanderten nur zu einem geringfügigen Anteil bis zu der Zellmembran und verblieben zu einem großen Teil im zellulären Plasma. In den elektrophysiologischen Studien an transfizierten HEK293 Zellen konnte bei beiden trunkierten Proteinen und bei dem durch die Spleiß-Variante veränderten Protein kein Natrium-Einwärtsstrom, ausgelöst durch Bindung von Acetylcholin, nachgewiesen werden. Hier zeigte sich somit ein vollkommener Funktionsverlust des α3β4-nAchR.

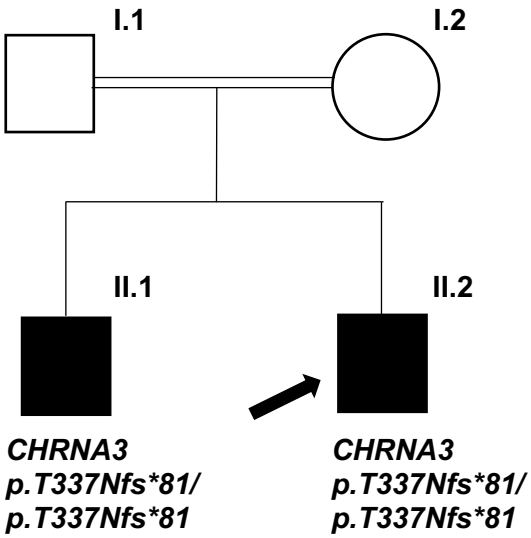

Abb. 3: Stammbaum der in Publikation C untersuchten Indexfamilie.
II.1: nicht-neurogene neurogene Blasenstörung, vesikoureteraler Reflux Grad 5, Hydronephrose, progressive Niereninsuffizienz, Mydriasis.
II.2: rezidivierende Harnwegsinfekte, verminderter Lichtreflex der Pupillen.
Der Indexpatient wird durch einen Pfeil markiert. Durch WES und Sanger-Sequenzierung identifizierte Mutationen sind angezeigt. CHRNA3, cholinergic receptor nicotinic alpha 3 subunit; T, Threonin; N, Asparagin; fs, frameshift.

1.4 Diskussion

Bei den in Publikation A-C untersuchten Familien war das Ziel, monogene Ursachen für die jeweiligen Fehlbildungen zu identifizieren.

Thema von **Publikation A** ist die Identifikation von *HSPA6* als ein rezessives Kandidatengen für Fehlbildungen im Zusammenhang mit der VATER/VACTERL Assoziation. Nicht nur seine embryonale Funktion, sondern auch das vorbeschriebene *TRAP1*, welches wie *HSPA6* für ein Hitzeschockprotein kodiert, legen seine ursächliche Rolle bei der Entstehung der beschriebenen Fehlbildungen nahe. Es fanden sich jedoch keine weiteren biallelischen Varianten in einer Kohorte von 167 Patienten mit ARM und VATER/VACTERL ähnlichem Phänotyp. Erstrebenswert wären eine Re-Sequenzierung in einer größeren Kohorte und tiefergehende Studien zur Beteiligung von

Hitzeschockproteinen an der Entstehung von ARM und Komponenten der VATER/VACTERL-Assoziation.
Die Mikrodeletion von *HSPA6* in Familie 1346 zeigt auf, dass auch CNVs zu biallelischen Krankheitsbildern als ursächliche Variante beitragen können. Darüber hinaus wäre es wünschenswert, die Beteiligung von CNVs bei Patienten zu untersuchen, bei denen keine monogenetische Ursache identifiziert werden kann.

Publikation B beschreibt das gleichzeitige Auftreten von EA/TEF und BO-Syndrom bei einem Patienten. Hier kann die *EYA1*-Mutation als alleinige Ursache gewertet werden, da *EYA1* im Hedgehog-Signalweg als upstream-Koordinator mit *FGF10* interagiert, welches im Tiermodell in die Entwicklung der Speiseröhre involviert ist (Korzh et al., 2011; Hajduk et al, 2010). Die *EYA1*-Mutation kann jedoch auch im Zusammenspiel mit Mutationen in weiteren Genen gesehen werden, welche im Hedgehog-Signalweg mit *EYA1* interagieren. Die *GLI3*-Mutation liegt hier in Kombination mit der *EYA1*-Mutation nur im Indexpatienten vor und suggeriert eine digenische Ursache für die EA/TEF beim Indexpatienten. Es könnte daher sein, dass die Kombination beider Varianten die Signalkaskade des Sonic hedgehog Signalwegs stört. Auch hier ist eine größere Kohorte mit EA/TEF und BO-Syndrom assoziierten Merkmalen wünschenswert, um einer möglichen Involvierung von *EYA1* in die Entstehung von EA/TEF nachzugehen. Einschränkend können ursächliche *de novo* Mutationen nicht ausgeschlossen werden. Diese hätten nur in einer Trio-basierten WES-Analyse identifiziert werden können.

In **Publikation C** werden rezessive (biallelische) Varianten in *CHRNA3* in drei nicht verwandten Familien beschrieben. CHRNA3 greift als Teil des α3β4-nAchR in die neuronale Regulation der Blase ein. Es wird sowohl in autonomen Ganglien als auch im Urothel exprimiert (Beckel et al., 2006; Fowler et al., 2008). Die Expression in autonomen Ganglien erklärt die dysautonomen Merkmale der betroffenen Patienten: diese reichen von der Fehlregulation der Blasenkontraktion und -relaxation bis zu einer Mydriasis. Die Übereinstimmung mit dem Mausmodell, in dem *Chrna*$^{-/-}$ Mäuse eine Megacystis, rezidivierende Harnwegsinfekte und Mydriasis zeigen, ist hier unübersehbar (Xu et al., 1999).
Für LUTO als Unterform von CAKUT sind bisher nur wenige Gene beschrieben worden, welche hauptsächlich in die Kontraktion von glatten Muskelzellen mittels Aktin oder in

synaptische neuronale Signalweiterleitung eingreifen (Weber et al., 2011; Wangler et al., 2014; Milewicz et al., 2010; Daly et al., 2010; Stuart et al., 2013). Einzig für das Gen *CHRM3*, welches wie *CHRNA3* in die neuronale Regulation der Blase involviert ist, sind ebenfalls Patienten mit persistierender Mydriasis beschrieben worden (Weber et al., 2011). Das unabhängige Auftreten der Mutationen in unterschiedlichen Familien und die funktionale Untersuchung der mutierten Proteine unterstützen *CHRNA3* als gutes Kandidatengen. Das Augenmerk sollte so nicht nur auf Gene gerichtet werden, die in die embryonale Entwicklung des Harntraktes oder in mechanische Vorgänge eingreifen, sondern auch auf Gene, die in die neuronale Regulation von beteiligten Strukturen involviert sind. Die hier untersuchten Patienten zeigen eine phänotypische Variabilität mit zum Teil nur versteckten oder fehlenden dysautonomen Merkmalen.
Voraussetzung für ein besseres Verständnis der Genotyp-Phänotyp-Korrelation ist die Identifikation weiterer Patienten mit *CHRNA3*-Mutationen.

1.5 Zusammenfassung

In den vorliegenden Studien (**Publikationen A-C**) untersuchte ich die genetischen Ursachen intestinaler Atresien und von CAKUT mittels Exom-Sequenzierung. Dabei standen monogene Erklärungsansätze im Mittelpunkt. *HSPA6* als Kandidatengen für ARM als Teil der VATER/VACTERL-Assoziation konnte nur in einer betroffenen Familie identifiziert werden. Im Fall des Patienten mit BO-Syndrom und EA/TEF suggeriert das Ergebnis ein digenisches Modell durch die Kombination von monoallelischen Varianten in *EYA1* und *GLI3*. In *CHRNA3* konnten wir für mehrere Familien mit gleichem Phänotyp ursächlich biallelische Varianten nachweisen. Funktionelle Studien unterstützen diese genetischen Ergebnisse. Im Kontext der neuronalen autonomen Regulation der Blase durch den α3β4-nAchR entsteht so eine pathophysiologische Sequenz, in deren Rahmen die neurogene Blasenstörung sekundär zu CAKUT führt. Die systematische Identifizierung weiterer genetischer Ursachen und weiterer Patienten mit ursächlichen Varianten in den beschriebenen Genen wird zu einem umfassenderen Verständnis der molekularen Vorgänge und der Krankheitsbilder führen. Im Fall der Patienten, die

ursächliche Varianten in *CHRNA3* tragen, ergeben sich gegebenenfalls, anders als bei Patienten mit mechanischen LUTOs, medikamentös therapeutische Optionen.
Darüber hinaus ist ein besseres Verständnis der genetischen Ursachen unerlässlich für die genetische Beratung von Patienten und deren Familien.

1.6 Literaturverzeichnis

Abdelhak S, Kalatzis V, Heilig R, Compain S, Samson D, Vincent C, Weil D, Cruaud C, Sahly I, Leibovici M, Bitner-Glindzicz M, Francis M, Lacombe D, Vigneron J, Charachon R, Boven K, Bedbeder P, van Regemorter N, Weissenbach J, Petit C. A human homologue of the Drosophila eyes absent gene underlies Branchio-Oto-Renal (BOR) syndrome and identifies a novel gene family. Nature Genetics. 1997; 15: 157-164

Balanescu RN, Topor R, Moga A. Anomalies associated with anorectal malformations.Chirurgia. 2013; 108: 38-42

Beckel JM, Kanai A, Lee SJ, de Groat WC, Birder LA. Expression of functional nicotinic acetylcholine receptors in rat urinary bladder epithelial cells. American journal of physiology-Renal physiology. 2006; 290: F103-110

Bekheirnia MR, Bekheirnia N, Bainbridge MN, Gu S, Akdemir ZHC, Gambin T, Janzen NK, Jhangiani SN, Muzny DM, Michael M, Brewer ED, Elenberg E, Kale AS, Riley AA, Swartz SJ, Scott DA, Yang Y, Srivaths PR, Wenderfer SE, Bodurtha J, Applegate CD, Velinov M, Myers A, Borovik L, Craigen WJ, Hanchard NA, Rosenfeld JA, Lewis RA, Gonzales ET, Gibbs RA, Belmont JW, Roth DR, Eng C, Braun MC, Lupski JR, Lamb DJ. Whole-exome sequencing in the molecular diagnosis of individuals with congenital anomalies of the kidney and urinary tract and identification of a new causative gene. Genetics in Medicine. 2017; 19: 412-420

Cuschieri A. Descriptive epidemiology of isolated anal anomalies: A survey of 4.6 million births in Europe. American Journal of Medical Genetics. 2001; 103: 207–215

Daly SB, Urquhart JE, Hilton E, McKenzie EA, Kammerer RA, Lewis M, Kerr B, Stuart H, Donnai D, Long DA, Burgu B, Aydogdu O, Derbent M, Garcia-Minaur S, Reardon W,

Gener B, Shalev S, Smith R, Woolf AS, Black GC, Newman WG. Mutations in *HPSE2* cause urofacial syndrome. American Journal of Human Genetics. 2010; 86: 963-969

De Jong EM, Douben H, Eussen BH, Felix JF, Wessels MW, Poddighe PJ, Nikkels PG, de Krijer RR, Tibboel D and de Klein A. 5q11.2 deletion in a patient with tracheal agenesis. European Journal of Human Genetics. 2010; 18: 1265-1268

Depaepe A, Dolk H and Lechat MF. The epidemiology of tracheo-esophageal fistula and oesophageal atresia in Europe. EUROCAT Working Group. Archives of Disease in Childhood. 1993; 68: 743-748

Desmet FO, Hamroun D, Lalande M and Collod-Béroud G, Claustres M and Béroud C. Human splicing finder: An online bioinformatics tool to predict splicing signals. Nucleic Acids Research. 2009; 37: e67

Fowler CJ, Griffiths D, de Groat WC. The neural control of micturition. Nature Reviews Neuroscience. 2008; 9: 453-466

Fraser FC, Sproude JR and Halal F. Frequency of the branchio-oto-renal (BOR) syndrome in children with profound hearing loss. American Journal of Medical Genetics. 1980; 7: 341-349

Hajduk P, Murphy P and Puri P. Fgf10 gene expression is delayed in the embryonic lung mesenchyme in the adriamycin mouse model. Pediatric Surgery International. 2010; 26: 23-27

Hildebrandt F, Heeringa SF, Rüschendorf F, Attansio M, Nürnberg G, Becker C, Seelow D, Huebner N, Chernin G, Vlangos CN, Zhou W, O'Toole JF, Hoskins BE, Wolf MTF, Hinkes BG, Chaib H, Ashraf S, Schoeb DS, Ovunc B, Allen SJ, Vega-Warner V, Wise E, Harville HM, Lyons RH, Washburn J, MacDonald J, Nürnberg P, Otto EA. A systematic approach to mapping recessive disease genes in individuals from outbred populations. Plos Genetics. 2009; 5: e1000353

Hoskins BE, Kramer CH, Silvius D, Zou D, Raymond RM, Orten DJ, Kimberling WJ, Smith RJ, Weil D, Petit C, Otto EA, Xu PX, Hildebrandt F. Transcription factor SIX5 is mutated

in patients with branchio-oto-renal syndrome. American Journal of Human Genetics. 2007; 80: 800-804

Korzh S, Winata CL, Zheng W, Yang S, Yin A, Ingham P, Korzh V and Gong Z. The interaction of epithelial Ihha and mesenchymal Fgf10 in zebrafish esophageal and swimbladder development. Developmental Biology. 2011; 359: 262-276

Krug P, Moriniére V, Marlin S, Koubi V, Gabriel HD, Colin E, Bonneau D, Salomon R, Antignac C and Heidet L. Mutation screening of the *EYA1*, *SIX1* and *SIX5* genes in a large cohort of patients harboring branchio-oto-renal syndrome calls into question the pathogenic role of SIX5 mutations. Human Mutation. 2011; 32: 183-190

Milewicz DM, Ostergaard JR, Ala-Kokko LM, Khan N, Grange DK, Mendoza-Londono R, Bradley TJ, Olney AH, Adès L, Maher JF, Guo D, Buja LM, Kim D, Hyland JC, Regalado ES. *De novo ACTA2* mutation causes a novel syndrome of multisystemic smooth muscle dysfunction. American Journal of Medical Genetics Part A. 2010; 152A: 2437-2443.

Motoyama J, Liu J, Mo R, Ding Q, Post M and Hui CC. Essential function of Gli2 and Gli3 in the formation of lung, trachea and oesophagus. Nature Genetics. 1998; 20: 54-57

Ruf RG, Xu PX, Silvius D, Otto EA, Beekmann F, Muerb UT, Kumar S, Neuhaus TJ, Kemper MJ, Raymond RM Jr, Brophy PD, Berkman J, Gattas M, Hyland V, Ruf EM, Schwartz C, Chang EH, Smith RJ, Stratakis CA, Weil D, Petit C, Hildebrandt F. SIX1 mutations cause branchio-oto-renal syndrome by disruption of EYA1-SIX1-DNA complexes. Proceedings of the National Academy of Sciences USA. 2004; 101: 8090-8095

Shapiro MB and Senapathy P: RNA splice junctions of different classes of eukaryotes: Sequence statistics and functional implications in gene expression. Nucleic Acids Research.1987; 15: 7155-7174

Saisawat P, Kohl S, Hilger AC, Hwang D-Y, Gee HY, Dworschak GC, Tasic V, Pennimpede T, Natarajan S, Sperry E, Matassa DS, Stajić N, Bogdanovic R, de Blaauw I, Marcelis CL, Wijers CH, Bartels E, Schmiedeke E, Schmidt D, Märzheuser S, Grasshoff-Derr S, Holland-Cunz S, Ludwig M, Nöthen MM, Draaken M, Brosens E, Heij H, Tibboel

D, Herrmann BG, Solomon BD, de Klein A, van Rooij IA, Esposito F, Reutter HM, Hildebrandt F. Whole exome resequencing reveals recessive mutations in TRAP1 in individuals with CAKUT and VACTERL association. Kidney International. 2014; 85: 1310–1317

Song MH, Kwon TJ, Kim HR, Jeon JH, Baek JI, Lee WS, Kim UK, Choi JY. Mutational analysis of EYA1, SIX1 and SIX5 genes and strategies for management of hearing loss in patients with BOR/BO syndrome. PLoS One. 2013; 8: e67236

Stockley TL, Mendoza-Londono R, Propst EJ, Sodhi S, Dupuis L and Papsin BC. A recurrent EYA1 mutation causing alternative RNA splicing in branchio-oto-renal syndrome: Implications for molecular diagnostics and disease mechanism. American Journal of Medical Genetics Part A. 2009; 149A: 322-327

Stoll C, Alembik Y, Dott B, Roth MP. Associated malformations in patients with anorectal anomalies. European Journal of Medical Genetics. 2007; 50: 281-290

Stuart HM, Roberts NA, Burgu B, Daly SB, Urquhart JE, Bhaskar S, Dickerson JE, Mermerkaya M, Silay MS, Lewis MA, Olondriz MB, Gener B, Beetz C, Varga RE, Gülpınar O, Süer E, Soygür T, Ozçakar ZB, Yalçınkaya F, Kavaz A, Bulum B, Gücük A, Yue WW, Erdogan F, Berry A, Hanley NA, McKenzie EA, Hilton EN, Woolf AS, Newman WG. LRIG2 mutations cause urofacial syndrome. American Journal of Human Genetics. 2013; 92: 259-264

van den Hondel D, Wijers CHW, van Bever Y, de Klein A, Marcelis CLM, de Blaauw I, Sloots CEJ, Ijsselstijn H. Patients with anorectal malformation and upper limb anomalies: Genetic evaluation is warranted. European Journal of Pediatrics. 2016; 175: 489–497

van der Ven AT, Vivante A, Hildebrandt F. Novel Insights into the Pathogenesis of Monogenic Congenital Anomalies of the Kidney and Urinary Tract. Journal of the American Society of Nephrology: JASN. 2018; 29: 36-50

Vincent C, Kalatzis V, Abdelhak S, Chaib H, Compain S, Helias J, Vaneecloo FM and Petit C. BOR and BO syndromes are allelic defects of EYA1. European Journal of Human Genetics. 1997; 5: 242-246

Vivante A, Kohl S, Hwang DY, Dworschak GC, Hildebrandt F. Single-gene causes of congenital anomalies of the kidney and urinary tract (CAKUT) in humans. Pediatric Nephrolology. 2014; 29: 695-704

Vogt EC: Congenital esophageal atresia. American Journal of Roentgenology.1929; 22: 463-465

Wangler MF, Gonzaga-Jauregui C, Gambin T, Penney S, Moss T, Chopra A, Probst FJ, Xia F, Yang Y, Werlin S, Eglite I, Kornejeva L, Bacino CA, Baldridge D, Neul J, Lehman EL, Larson A, Beuten J, Muzny DM, Jhangiani S; Baylor-Hopkins Center for Mendelian Genomics, Gibbs RA, Lupski JR, Beaudet A. Heterozygous de novo and inherited mutations in the smooth muscle actin (ACTG2) gene underlie megacystis-microcolon-intestinal hypoperistalsis syndrome. PLoS genetics. 2014; 10: e1004258

Weber S, Thiele H, Mir S, Toliat MR, Sozeri B, Reutter H, Draaken M, Ludwig M, Altmüller J, Frommolt P, Stuart HM, Ranjzad P, Hanley NA, Jennings R, Newman WG, Wilcox DT, Thiel U, Schlingmann KP, Beetz R, Hoyer PF, Konrad M, Schaefer F, Nürnberg P, Woolf AS. Muscarinic Acetylcholine Receptor M3 Mutation Causes Urinary Bladder Disease and a Prune-Belly-like Syndrome. American Journal of Human Genetics. 2011; 89: 668-674

Received: 30 December 2018 | Revised: 21 February 2019 | Accepted: 3 March 2019

DOI: 10.1002/bdr2.1493

WILEY Birth Defects Research

ORIGINAL ARTICLE

HSPA6: A new autosomal recessive candidate gene for the VATER/VACTERL malformation spectrum

Franziska Kause[1] | Rong Zhang[1,2] | Michael Ludwig[3] | Eberhard Schmiedeke[4] | Anke Rissmann[5] | Holger Thiele[6] | Janine Altmueller[6,7] | Stefan Herms[2,8,9] | Alina C. Hilger[1,10] | Friedhelm Hildebrandt[11] | Heiko Reutter[1,12]

[1]Institute of Human Genetics, University of Bonn, Bonn, Germany

[2]Department of Genomics, Life & Brain Center, Bonn, Germany

[3]Department of Clinical Chemistry and Clinical Pharmacology, University of Bonn, Bonn, Germany

[4]Clinic for Paediatric Surgery and Paediatric Urology, Klinikum Bremen-Mitte, Bremen, Germany

[5]Malformation Monitoring Centre Saxony-Anhalt, Medical Faculty, Otto-von-Guericke University, Magdeburg, Germany

[6]Cologne Center for Genomics, University of Cologne, Cologne, Germany

[7]Center for Molecular Medicine Cologne (CMMC), University of Cologne, Cologne, Germany

[8]Institute of Medical Genetics and Pathology, University Hospital Basel, Basel, Switzerland

[9]Department of Biomedicine, Human Genomics Research Group, University of Basel, Basel, Switzerland

[10]Children's Hospital, University of Bonn, Bonn, Germany

[11]Division of Nephrology, Boston Children's Hospital, HMS, Boston, Massachusetts

[12]Department of Neonatology and Pediatric Intensive Care, Children's Hospital, University of Bonn, Bonn, Germany

Correspondence
Franziska Kause, Institute of Human Genetics, University of Bonn, Bonn, Germany.
Email: s4frkaus@uni-bonn.de

Funding information
BONFOR/ University of Bonn, Grant/Award Numbers: O-149.0096, O.149.0123; Deutsche Forschungsgemeinschaft, Grant/Award Number: RE 1723/4-1; Else-Kröner-Fresenius-Stiftung, Grant/Award Number: 2014_A14; National Institutes of Health, Grant/Award Number: DK076683

Background: The VATER/VACTERL association refers to the nonrandom co-occurrence of at least three of the following component features (CFs): vertebral defects (V), anorectal malformations (ARM) (A), cardiac defects (C), tracheoesophageal fistula with or without esophageal atresia (TE), renal malformations (R), and limb defects (L). Patients presenting with two CFs have been termed VATER/VACTERL-like phenotypes.

Methods: We surveyed the exome for recessive disease variants in three affected sib-pairs. Sib-pair 971 consisted of two brothers with ARM and additional hydronephrosis in one brother. Sib-pair 1098 consisted of two sisters with ARM. In family 1346, the daughter presented with ARM and additional hypoplasia of both small fingers and ankyloses. Her brother presented with unilateral isolated radial hypoplasia. Sib-pairs 971 and 1346 resembled a VATER/VACTERL-like phenotype.

Results: We detected a novel maternally inherited missense variant (c.1340G > T) and a rare paternally inherited deletion of the trans-allele in *HSPA6* in both siblings of family 1346. HSPA6 belongs to the heat shock protein (HSP) 70 family. Re-sequencing of *HSPA6* in 167 patients with VATER/VACTERL and VATER/VACTERL-like phenotypes did not reveal any additional bi-allelic variants.

Conclusions: Until now, only TNF-receptor associated protein 1 (*TRAP1*) had been reported as an autosomal recessive disease-gene for the VATER/VACTERL association. *TRAP1* belongs to the heat shock protein 90 family (HSP90). Both *Hsp70* and *Hsp90* genes have been shown to be important embryonic drivers in the formation of mouse embryonic forelimb tissue. Our results suggest *HSPA6* as a new candidate gene in VATER/VACTERL-like phenotypes.

KEYWORDS

anorectal malformations, autosomal recessive inheritance, *HSPA6*, VATER/VACTERL association, whole-exome sequencing

1 | INTRODUCTION

Anorectal malformations (ARMs) are rare disorders of the embryonic distal hindgut. They occur in about 1 in 4.000 live births (Cuschieri, 2001; Bartels et al., 2012). They are caused by defective differentiation of the primitive hindgut (Matsumaru et al., 2015). ARM present with a broad phenotypic spectrum ranging from perineal fistula to severe cloacal malformations. For phenotypic classification of ARM, the Krickenbeck classification system is usually applied (Holschneider et al., 2005). Around 60% of ARM patients present with co-occurring congenital malformations, most of which belong to the congenital anomaly spectrum of the VATER/VACTERL association. The VATER/VACTERL association refers to the nonrandom co-occurrence of at least three of the following component features (CFs): vertebral defects (V), ARMs (A), cardiac defects (C), tracheoesophageal fistula with or without esophageal atresia (TE), renal malformations (R), and limb defects (L) (Belloni et al., 2000; Kohlhase, Wischermann, Reichenbach, Froster, & Engel, 1998; Solomon et al., 2014). Patients presenting with two CFs have been termed VATER/VACTERL-like phenotypes. ARM in combination with major upper limb malformations as defined by van den Hondel et al. occurs in about 6% of ARM patients (van den Hondel et al., 2016).

After the detection of causative copy number variations in patients with ARM and ARM as part of their VATER/VACTERL association (Bartels et al., 2011; Dworschak et al., 2013; Schramm, Draaken, Bartels, Boemers, Aretz, et al., 2011; Schramm, Draaken, Bartels, Boemers, Schmiedeke, et al., 2011; Schramm, Draaken, Tewes, et al., 2011) Saisawat et al. (2014) were the first who identified a recessive disease-gene, namely TNF-receptor associated protein 1 (*TRAP1*), in patients with VATER/VACTERL association and congenital anomalies of the kidney and urinary tract (CAKUT) (Saisawat et al., 2014). *TRAP1*, located on 16p13.3, belongs to the heat shock protein 90 family (HSP90) (Chen, Piel, Gui, Bruford, & Monteiro, 2005).

Here, we aimed to identify rare autosomal recessive disease-genes for isolated ARM or ARM as part of VATER/VACTERL-like phenotypes. For this purpose, we performed whole-exome sequencing (WES) in three affected sib-pairs and their healthy parents and re-sequenced the top candidate gene in 167 patients with VATER/VACTERL and VATER/VACTERL-like phenotypes.

2 | MATERIALS AND METHODS

2.1 | Patients, controls, and DNA isolation

Patients and families were recruited through the German network for congenital uro-rectal malformations (CURE-Net, www.cure-net.de) and the great-consortium (genetic risk of esophageal atresia, www.great-konsortium.de). Written informed consent was obtained from every family. The study was approved by the Ethics Committee of the Medical Faculty of the University of Bonn (Lfd. Nr. 073/12 & 146/12). Genomic DNA was isolated from whole blood using the Chemagic DNA Blood Kit special (Chemagen, Baesweiler, Germany). Genomic DNA from saliva samples was isolated with the Oragene DNA Kit (DNA Genotek Inc., Kanata, Canada).

Our study included three affected sib-pairs and their healthy parents. In Family 971, two affected brothers (971_II.1, 971_II.2) presented with ARM and additional hydronephrosis in 971_II.1 and ARM in form of a perineal fistula in 971_II.2. Sib-pair 1098 consisted of two affected sisters (1098_II.1, 1098_II.2) presenting with ARM in form of a perineal fistula. In Family 1346, the affected daughter (1346_II.1) presented with ARM in form of a perineal fistula and additional hypoplasia of both small fingers and ankyloses. Her brother (1346_II.2) presented with unilateral isolated radial hypoplasia. Hence, Sib-pairs 971 and 1346 resemble the phenotypic spectrum of a VATER/VACTERL-like phenotype (Table 1).

For re-sequencing of the top candidate gene, we chose 167 patients presenting with VATER/VACTERL and VATER/VACTERL-like phenotypes.

2.2 | Whole-exome sequencing (WES) and data analysis

WES was performed at the Next Generation Sequencing Laboratory of the Institute of Human Genetics of the University of Bonn. For the enrichment of exonic and adjacent intronic sequences from genomic DNA, the NimbleGen SeqCap EZ Human Exome Library v2.0 enrichment kit was used. WES was performed on an Illumina HiSeq2500 sequencer using a 100 bp paired-end read protocol, following the manufacturer's recommendations. Data analysis and filtering of mapped target sequences was accomplished with "Varbank" exome and genome analysis pipeline v.2.1 (https://varbank.ccg.uni-koeln.de). We especially filtered for high-quality (coverage of more than six reads, a minimum quality score of 10, VQSLOD greater then −8) and rare (allele frequency < 0.5%) autosomal variants. In Sib-pair 971 with two affected brothers, we also filtered for X-chromosomal recessive variants. A detailed description of filter criteria has been described elsewhere (Zhang et al., 2016).

2.3 | Confirmation of variants detected by WES

Variants identified by WES and called to be possibly causative were amplified from the DNA by polymerase chain reaction (PCR). Automated sequence analysis was carried out using standard procedures. From the UCSC Human Genome Browser (https://genome.ucsc.edu/) and Ensembl (http://www.ensembl.org/index.html) genomic and cDNA sequences were obtained to compile primers. PCR products

TABLE 1 Phenotypic features of the patients of Family 1098, 971, and 1346

Family number	Patient	Anorectal malformation	Other features
1098	II.1	Anorectal malformation in form of a perineal fistula	
	II.2	Anorectal malformation in form of a perineal fistula	
971	II.1	Anorectal malformation	Hydronephrosis, left
	II.2	Anorectal malformation in form of a perineal fistula	
1346	II.1	Anorectal malformation in form of a perineal fistula	Hypoplasia and ankyloses of both small fingers
	II.2		Radial hypoplasia

were subjected to direct automated BigDye Terminator sequencing (3130XL Genetic Analyzer, Applied Biosystems, Foster City, CA). Both strands from each amplicon were sequenced and presence of the variants in each family was confirmed by sequencing the respective PCR product (primer sequences are available upon request).

2.4 | Re-sequencing of candidate gene *HSPA6*

For the amplification of DNA, PCR primers were designed for exon 1 of *HSPA6*. The resultant PCR products were referred to direct automated sequencing with the 3130XL Genetic Analyzer (Applied Biosystems).

2.5 | Quantitative polymerase chain reaction

Quantitative PCR (qPCR) was performed on a Roche Light Cycler 480 II (Roche, Basel, Switzerland) with Roche Light Cycler Sybr Green I Master Mix. Each assay included the respective DNA specimen at a final concentration of 10 ng/μL in triplicate. Reaction mixtures (10 μL) contained 0.2 mmol of each primer and 5 μL of SYBR Green Master Mix (Roche) with cycling conditions as follows: initiation 50°C for 2 min, denaturation 95°C for 10 min, followed by 40 cycles at 95°C for 15 s, and a combined annealing and extension step at 64°C for 60 s. The threshold cycle (Ct) values were normalized using the Ct value of three reference genes (*BNC1*, *CFTR*, and *RNAseP* subunit p38) for each DNA sample. Relative quantification was done using the comparative Ct method normalizing to the mother as a control sample, since she was found to be heterozygous for variant c.1340G > T and therefore could not carry a deletion of this region (primer sequences are available upon request).

2.6 | In silico prediction of variants

To predict the effect of the variants on the function and structure of the encoded proteins, we used seven online prediction tools (SIFT [http://sift.jcvi.org/], Mutation Assessor 3 [http://mutationassessor.org/r3/], fathmm [http://fathmm.biocompute.org.uk/], PROVEAN [http://provean.jcvi.org/index.php], Mutation Taster [http://www.mutationtaster.org/], PolyPhen-2 [http://genetics.bwh.harvard.edu/pph2/], and the CADD-PHRED-score [http://cadd.gs.washington.edu/home]).

3 | RESULTS

Using WES, we investigated three affected sib-pairs and their healthy parents for autosomal recessive disease variants. In the case of affected male brothers, we also surveyed the exome for X-chromosomal disease variants (Table 1). Analysis of the WES-data revealed two candidate genes in Family 971 and Family 1346. No X-chromosomal disease variant was found in Sib-pair 971. No autosomal recessive disease variants were found in Sib-pair 1098.

3.1 | Sib-pair #971

We detected two possible disease-causing variants in *ITSN2*, suggesting a compound heterozygous background in the affected brothers 971_II.1 and 971_II.2 (c.1442 T > A and c.4367A > G, according to ENSEMBL GRCh37/hg19 transcript ENST00000355123). The variant c.1442 T > A (p.Ile481Asn, ENSP00000347244) was predicted to be deleterious by five out of seven in silico prediction tools (deleterious in SIFT [score: 0], medium functional impact by Mutation Assessor [FI-score: 2.175], tolerated in fathmm [score: 0.08], deleterious in PROVEAN [score: −5.80], disease-causing in Mutation Taster [*p* value: 1], probably damaging by PolyPhen-2 [humvar score 0.996], CADD score of 25.4). In contrast, for the second variant c.4367A > G (single nucleotide polymorphism [SNP]: rs139986826; p.Asn1456Ser [ENSP00000347244]), the amino acid change was predicted to be deleterious by two out of the seven in silico prediction tools (tolerated in SIFT [score 0.64], low functional impact in Mutation Assessor [score: 1.01], tolerated in fathmm [score: −0.26], deleterious in PROVEAN [score: −3.67], disease-causing in Mutation Taster [*p* value: 0.926], benign in PolyPhen-2 [humvar score 0.009], CADD-PHRED-score of 17.3). The zebrafish (*Danio rero*) and the green spotted pufferfish (*Tetraodon nigroviridis*) present with a Serine at the homologous position. Previously, high-throughput sequencing revealed recessive mutations of *ITSN2* as causing nephrotic syndrome (NS) in humans (Ashraf et al., 2018). Neither of the two brothers (971_II.1 and 971_II.2) presented with symptoms of NS. Of course, we cannot exclude that the two brothers will manifest NS in the future. However, none of the initially reported patients with NS and recessive disease variants in *ITSN2* exhibited any CF of the VATER/VACTERL association spectrum. Hence, we assume that the variants in *ITSN2* are probably not disease causing for the development of ARM in an autosomal recessive context in

our patients. Screening for X-linked variants did not reveal any disease variant for the two brothers.

3.2 | Sib-pair #1346

In Sib-pair 1346, WES revealed an apparent homozygous mutation in *heat shock protein family A (HSP70) member 6* (*HSPA6* or *HSP70B'*, here referred to as *HSPA6*) (c.1340G > T, according to ENSEMBL GRCh37/hg19 transcript ENST00000309758) in exon 1. Polyphen2, SIFT, Mutation Taster, Mutation Assessor and PROVEAN predicted the mutation to be damaging (Table 2). With a CADD-score of 25.5, it is among 1% of the most deleterious variants in the human genome. The *HSPA6* p.Gly447Val mutation (SNP: rs56366425) alters a highly conserved amino acid. It is conserved throughout the species to *Saccharomyces cerevisiae* with no orthologue in mice (Leung, Hall, Rajendran, Spurr, & Lim, 1992) (Table 2). Segregation analysis revealed a heterozygous variant in the mother. The father presented with a wild type allele and qPCR revealed a deletion of *HSPA6* on the trans-allele. Both children inherited variant c.1340G > T from their mother. They also inherited a microdeletion harboring *HSPA6* from their father on the trans-allele (Figure 1). In our in-house control cohort, 1 out of 1.320 healthy individuals carried a deletion at the *HSPA6* locus (data not shown). Copy number variations (CNVs) in our in-house controls were identified via the human Infinium Omni 2.5 BeadChip (Illumina, San Diego, CA) and evaluated with the Illumina Genome Viewer program. The frequency of 1 in 1.320 (≈0.0008) of the observed deletion in our population-based control cohort is clearly below the population-based frequency of ARM and ARM as part of the VATER/VACTERL association in a recessive disease-model (1 in 4.000 and 1 in 40.000, respectively; Cuschieri, 2001; Bartels et al., 2012). *HSPA6* is a member of the HSP70 protein family coding for HSPs throughout the human organism (Leung, Rajendran, Monfries, Hall, & Lim, 1990). It contains only one exon of 2.731 base pairs (according to ENSEMBL GRCh37/hg19 transcript ENST00000309758), a conserved N-terminal nucleotide-binding domain as well as a C-terminal peptide substrate-binding domain (Wisniewska et al., 2010).

To follow up on this finding, we re-sequenced *HSPA6* in 167 patients with VATER/VACTERL or VATER/VACTERL-like phenotypes resembling the phenotypes of patients 1346_II.1 and 1346_II.2 (ARM and limb malformation).

Sanger sequencing revealed four exonic heterozygous missense variants with minor allele frequencies (MAF) > 0.08. Additionally, we found three synonymous rare exonic variants (MAF < 0.08) and two exonic synonymous common SNPs were detected. In the untranslated region, three common SNPs as well as one rare variant (MAF unknown) were detected. Overall, we did not detect any further recessive disease variants in the investigated cohort.

TABLE 2 Mutations in HSPA6 (NM_002155.3) in patients 1346_II.1 and 1346_II.2 with anorectal malformations and limb deformities

Nucleotide alteration/deletion (zygosity)	Exon	Amino acid change	MutT	PP2	SIFT	MutA	FATHMM	PROVEAN	CADD v1.3	Segregation/State of alleles	CP	Gg	Xt	Dr	Ci	Ce	Dm	Sc
c.1340G > T (h)	1	G447 V	D.C.	1.000	D	4.085	T	D	25.5	Maternal inheritance	G	G	G	G	G	G	G	G
Deletion (h)	1	–	–	–	–	–	–	–	–	Paternal inheritance	–	–	–	–	–	–	–	–

Note. CADD v1.3: combined annotation dependent depletion v1.3 PHRED like scaled C-score; *Ce*: *Caenorhabditis elegans*; *Ci*: *Ciona intestinalis*; *Cp*: *Cavia porcellus*; D: deleterious; D.C.: disease causing; *Dm*: *Drosophila melanogaster*; *Dr*: *Danio rerio*; FATHMM: functional analysis through Hidden Markov models (v2.3); G: Glycine; *Gg*: *Gallus gallus*; h: heterozygous; MutA: Mutation Assessor 3 functional impact score; MurT: Mutation Taster prediction class; PROVEAN: protein variation effect analyzer; PP2: PolyPhen2 humvar score; *Sc*: *Saccharomyces cervisiae*; SIFT: sorting intolerant from tolerant prediction class; T: tolerated; V: valine; *Xt*: *Xenopus tropicalis*.

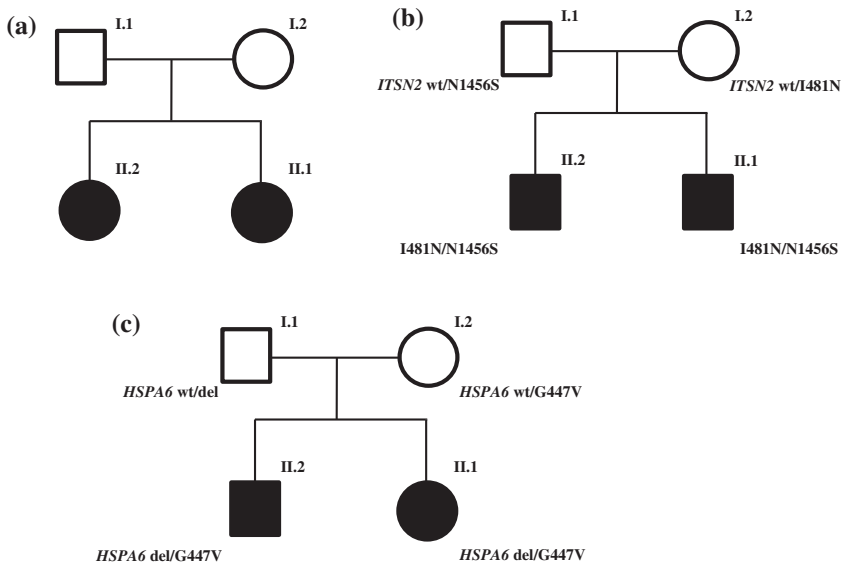

FIGURE 1 Pedigrees of the families. (a) 1098_II.1 and 1098_II.2 presented both with ARM in form of a perineal fistula. (b) 971_II.1 presented with ARM and left hydronephrosis. 971_II.2 presented with ARM in form of a perineal fistula. (c) 1346_II.1 presented with ARM in form of a perineal fistula, hypoplasia and ankylosis of both small fingers. 1346_II.2 presented with isolated radial hypoplasia. The presence or absence of genetic variants detected by whole-exome sequencing and (quantitative) polymerase chain reaction are indicated. Members affected with anorectal or skeletal malformations are shown in black, while unaffected members are shown in white. Males and females are represented in squares and circles, respectively. del: deletion; *HSPA6*: heat shock 70kD protein 6; *ITSN2*: intersection 2; wt: wild type

4 | DISCUSSION

Our WES analysis identified compound heterozygous variants in an affected sib-pair with congenital anomalies of the VATER/VACTERL association spectrum. Both carried a novel missense variant c.1340G > T in *HSPA6*, inherited from their healthy mother and a deletion of *HSPA6* on the trans-allele inherited from their healthy father. The variant was absent in the gnomAD browser beta (http://gnomad.broadinstitute.org/ [Lek et al., 2016] or in the exome variant server database (Exome Variant Server, NHLBI GO Exome Sequencing Project (ESP), Seattle, WA (URL: http://evs.gs.washington.edu/EVS/) [12/2018]). In the ExAC Browser (Beta) (http://exac.broadinstitute.org/ [Lek et al., 2016]) the allele count for this variant was 36 in 121098 alleles without any homozygous individuals listed and with an allele frequency of about 0.0003. Fifteen studies listed in the database of genomic variants describe the loss of genome sequences in the region of *HSPA6* (http://dgv.tcag.ca/dgv/app/home?ref=; (MacDonald, Ziman, Yuen, Feuk, & Scherer, 2014)) without mentioning population-based frequencies. Here, we investigated a healthy control cohort of 1.320 individuals and found one of these 1.320 healthy individuals to carry a deletion at the *HSPA6* locus revealing a population-based frequency clearly below the population-based frequency of ARM and ARM as part of the VATER/VACTERL association in a recessive disease-model (1 in 4.000 and 1 in 40.000 live births, respectively; Cuschieri, 2001; Bartels et al., 2012). Screening 167 patients with VATER/VACTERL or VATER/VACTERL-like phenotypes resembling the phenotypes of patients 1346_II.1 and 1346_II.2 (ARM and limb malformation) did not reveal any recessive disease variants.

The highly conserved *HSPA6* gene (Daugaard, Rohde, & Jäättelä, 2007; Gupta & Golding, 1993) belongs to the multigene HSP family A (HSP70). Little is known about the function of *HSPA6*, a gene present in the human genome but absent from mouse and rat (Deane & Brown, 2018). To our knowledge, there are no animal models for functional screening of the orthologous gene although it is present in other vertebrates and species such as frog, fruit fly, or yeast (Table 2). Emerging research suggests the HSPA6 protein to be involved in apoptotic response and cellular differentiation and to contribute to protection of differentiated human neuronal cells from cellular stress (Deane & Brown, 2018). Only when induced after severe stress events (Parsian et al., 2000), it functions as a secondary responder to proteotoxic stress and maintains cellular survival by directly binding to Apaf-1 and inhibiting the assembly of a functional apoptosome (Beere et al., 2000; Noonan, Place, Giardina, & Hightower, 2007). The involvement of HSP70s in regulation of the cell cycle and apoptotic pathways is essential for human embryonal development as they protect embryonal cells from cell stress such as hyperthermia or chemical teratogens (Luft & Dix, 1999). This is supported by the identification of *HSPA6* in

context of preterm birth in genetic association studies (Ryckman et al., 2010). Noonan et al. demonstrated that a knockdown of *HSPA6* in human colon cell lines leads to cell death induced by proteasome inhibition (Noonan, Fournier, & Hightower, 2008). Furthermore, expression patterns of members of the HSP70 family and of the HSP90 family during embryo development in mice show their involvement and protective role in limb formation (Zhu et al., 2012). Interestingly, different HSPs show a characteristic correlation with the developmental phases in mice embryos. As bi-allelic mutations in the *TRAP1* gene (member of the HSP90 family) cause CAKUT and malformations of the VATER/VACTERL association spectrum, one might assume a similar effect of mutations in *HSPA6* being part of a tight interaction network of HSPs during chaperone activity and transcriptional regulation (Mayer & Bukau, 2005; Prodromou, 2016).

In summary, our results suggest that bi-allelic recessive mutations in *HSPA6* contribute to congenital anorectal and limb malformations as part of the VATER/VACTERL association spectrum. Our analysis focused on exome-variants generated by WES in three affected sib-pairs and their healthy parents. Our finding of a paternally inherited deletion of *HSPA6* in sib-pair 1346 may be further explored by using CNV analysis. This may help detecting autosomal recessive microdeletions or duplications in Sib-pair 1098. Further studies are needed to explore how *HSP70*s influence the development of ARMs and features of the VATER/VACTERL association.

ACKNOWLEDGMENTS

We thank all patients and their families for their participation, as well as the German patient organizations for patients with ARMs (SoMA e.V.) and esophageal atresia with or without tracheoesophageal fistula (EA/TEF) (KEKS e.V.) for their assistance with recruitment. F.K. was supported by a stipend of the University of Bonn, BONFOR (grant no. O-149.0096). A.C.H. was supported by a stipend of the University of Bonn, BONFOR (grant no. O.149.0123). F.H. was supported by National Institutes of Health (grant no. DK076683). H.R. and M.L. are supported by the German Research Foundation (Deutsche Forschungsgemeinschaft, DFG) (grant no. RE 1723/4-1). H.R. and H.T. are further supported by a grant of the Else-Kröner-Fresenius-Stiftung (EKFS, grant no. 2014_A14).

ORCID

Franziska Kause https://orcid.org/0000-0002-0074-8962
Heiko Reutter https://orcid.org/0000-0002-3591-5265

REFERENCES

Ashraf, Z., Kudo, H., Rao, J., Kikuchi, A., Widmeier, E., Lawson, J. A., … Hildebrandt, F. (2018). Mutations in six nephrosis genes delineate a pathogenic pathway amenable to treatment. *Nature Communications*, *9*(1), 1960. https://doi.org/10.1038/s41467-018-04193-w

Bartels, E., Draaken, M., Kazmierczak, B., Spranger, S., Schramm, C., Baudisch, F., … Reutter, H. (2011). De novo partial trisomy 18p and partial monosomy 18q in a patient with anorectal malformation. *Cytogenetic and Genome Research*, *134*(3), 243–248. https://doi.org/10.1159/000328833

Bartels, E., Jenetzky, E., Solomon, B. D., Ludwig, M., Schmiedeke, E., Grasshoff-Derr, S., … Zwink, N. (2012). Inheritance of the VATER/VACTERL association. *Pediatric surgery international*, *28*(7), 681–685. https://doi.org/10.1007/s00383-012-3100-z

Beere, H. M., Wolf, B. B., Cain, K., Mosser, D. D., Mahboubi, A., Kuwana, T., … Green, D. R. (2000). Heat-shock protein 70 inhibits apoptosis by preventing recruitment of procaspase-9 to the Apaf-1 apoptosome. *Nature Cell Biology*, *2*, 469–475. https://doi.org/10.1038/35019501

Belloni, E., Martucciello, G., Verderio, D., Ponti, E., Seri, M., Jasonni, V., … Scherer, S. W. (2000). Involvement of the HLXB9 Homeobox gene in Currarino syndrome. *American Journal of Human Genetics*, *66*(1), 312–319. https://doi.org/10.1086/302723

Chen, B., Piel, W. H., Gui, L., Bruford, E., & Monteiro, A. (2005). The HSP90 family of genes in the human genome: Insights into their divergence and evolution. *Genomics*, *86*(6), 627–637. https://doi.org/10.1016/j.ygeno.2005.08.012

Cuschieri, A. (2001). Descriptive epidemiology of isolated anal anomalies: A survey of 4.6 million births in Europe. *American Journal of Medical Genetics*, *103*(3), 207–215. https://doi.org/10.1002/ajmg.1532

Daugaard, M., Rohde, M., & Jäättelä, M. (2007). The heat shock protein 70 family: Highly homologous proteins with overlapping and distinct functions. *FEBS Letters*, *581*(19), 3702–3710. https://doi.org/10.1016/j.febslet.2007.05.039

Deane, C. A. S., & Brown, I. R. (2018). Knockdown of HSPA6 (Hsp70B') and HSPA1A (Hsp70-1) sensitizes differentiated human neuronal cells to cellular stress. *Neurochemical Research*, *43*(2), 340–350. https://doi.org/10.1007/s11064-017-2492-z

Dworschak, G. C., Draaken, M., Marcelis, C., De Blaauw, I., Pfundt, R., Van Rooij, I. A. L. M., … Reutter, H. (2013). De novo 13q deletions in two patients with mild anorectal malformations as part of VATER/VACTERL and VATER/VACTERL-like association and analysis of EFNB2 in patients with anorectal malformations. *American Journal of Medical Genetics Part A*, *161*(12), 3035–3041. https://doi.org/10.1002/ajmg.a.36153

Gupta, R., & Golding, G. (1993). Evolution of HSP70 gene and its implications regarding relationships between archaebacteria, eubacteria, and eukaryotes. *Journal of Molecular Evolution*, *37*(6), 573–582. https://doi.org/10.1007/bf00182743

Holschneider, A., Hutson, J., Peña, A., Beket, E., Chatterjee, S., Coran, A., … Kunst, M. (2005). Preliminary report on the International conference for the development of standards for the treatment of anorectal malformations. *Journal of Pediatric Surgery*, *40*(10), 1521–1526. https://doi.org/10.1016/j.jpedsurg.2005.08.002

Kohlhase, J., Wischermann, A., Reichenbach, H., Froster, U., & Engel, W. (1998). Mutations in the SALL1 putative transcription factor gene cause Townes-Brocks syndrome. *Nature Genetics*, *18*, 81–83. https://doi.org/10.1038/ng0198-81

Lek, M., Karczewski, K. J., Minikel, E. V., Samocha, K. E., Banks, E., Fennell, T., … MacArthur, D. G. (2016). Analysis of protein-coding genetic variation in 60,706 humans. *Nature*, *536*(7616), 285–291. https://doi.org/10.1038/nature19057

Leung, T. K., Rajendran, M. Y., Monfries, C., Hall, C., & Lim, L. (1990). The human heat-shock protein family. Expression of a novel heat-inducible HSP70 (HSP70B') and isolation of its cDNA and genomic DNA. *The Biochemical Journal*, *267*(1), 125–132. https://doi.org/10.1042/bj2670125

Leung, T. K. C., Hall, C., Rajendran, M., Spurr, N. K., & Lim, L. (1992). The human heat-shock genes HSPA6 and HSPA7 are both expressed and localize to chromosome 1. *Genomics*, *12*(1), 74–79. https://doi.org/10.1016/0888-7543(92)90409-L

Luft, J., & Dix, D. (1999). Hsp70 expression and function during embryogenesis. *Cell Stress & Chaperones*, *4*, 162–170.

MacDonald, J. R., Ziman, R., Yuen, R. K. C., Feuk, L., & Scherer, S. W. (2014). The database of genomic variants: A curated collection of structural variation in the human genome. *Nucleic Acids Research*, *42*(Database issue), D986–D992. https://doi.org/10.1093/nar/gkt958

Matsumaru, D., Murashima, A., Fukushima, J., Senda, S., Matsushita, S., Nakagata, N., … Yamada, G. (2015). Systematic stereoscopic analyses for cloacal development: The origin of anorectal malformations. *Scientific Reports*, *5*, 13943. https://doi.org/10.1038/srep13943

Mayer, M. P., & Bukau, B. (2005). Hsp70 chaperones: Cellular functions and molecular mechanism. *Cellular and Molecular Life Sciences*, *62*(6), 670–684. https://doi.org/10.1007/s00018-004-4464-6

Noonan, E., Fournier, G., & Hightower, L. (2008). Surface expression of Hsp70B' in response to proteasome inhibition in human colon cells. *Cell Stress and Chaperones*, *13*(1), 105–110. https://doi.org/10.1007/s12192-007-0003-3

Noonan, E., Place, R., Giardina, C., & Hightower, L. (2007). Hsp70B' regulation and function. *Cell Stress & Chaperones*, *12*(3), 219–229. https://doi.org/10.1379/csc-278.1

Parsian, A. J., Sheren, J. E., Tao, T. Y., Goswami, P. C., Malyapa, R., Van Rheeden, R., … Hunt, C. R. (2000). The human Hsp70B gene at the HSPA7 locus of chromosome 1 is transcribed but non-functional. *Biochimica et Biophysica Acta*, *1494*(1–2), 201–205.

Prodromou, C. (2016). Mechanisms of Hsp90 regulation. *Biochemical Journal*, *473*(16), 2439–2452. https://doi.org/10.1042/bcj20160005

Ryckman, K. K., Morken, N.-H., White, M. J., Velez, D. R., Menon, R., Fortunato, S. J., … Jacobsson, B. (2010). Maternal and fetal genetic associations of PTGER3 and PON1 with preterm birth (genetics of preterm birth). *PLoS ONE*, *5*(2), e9040. https://doi.org/10.1371/journal.pone.0009040

Saisawat, P., Kohl, S., Hilger, A. C., Hwang, D.-Y., Gee, H. Y., Dworschak, G. C., … Hildebrandt, F. (2014). Whole exome resequencing reveals recessive mutations in TRAP1 in individuals with CAKUT and VACTERL association. *Kidney International*, *85*(6), 85–1317. https://doi.org/10.1038/ki.2013.417

Schramm, C., Draaken, M., Bartels, E., Boemers, T. M., Aretz, S., Brockschmidt, F. F., … Reutter, H. (2011). De novo microduplication at 22q11.21 in a patient with VACTERL association. *European Journal of Medical Genetics*, *54*(1), 9–13. https://doi.org/10.1016/j.ejmg.2010.09.001

Schramm, C., Draaken, M., Bartels, E., Boemers, T. M., Schmiedeke, E., Grasshoff-Derr, S., … Reutter, H. (2011). De novo duplication of 18p11.21-18q12.1 in a female with anorectal malformation. *American Journal of Medical Genetics. Part A*, *155A*(2), 445–449. https://doi.org/10.1002/ajmg.a.33820

Schramm, C., Draaken, M., Tewes, G., Bartels, E., Schmiedeke, E., Märzheuser, S., … Ludwig, M. (2011). Autosomal-dominant non-syndromic anal atresia: Sequencing of candidate genes, array-based molecular karyotyping, and review of the literature. *European Journal of Pediatrics*, *170*(6), 741–746. https://doi.org/10.1007/s00431-010-1332-2

Solomon, B. D., Baker, L. A., Bear, K. A., Cunningham, B. K., Giampietro, P. F., Hadigan, C., … Warren-Mora, N. (2014). An approach to the identification of anomalies and etiologies in neonates with identified or suspected VACTERL (vertebral defects, anal atresia, tracheo-esophageal fistula with esophageal atresia, cardiac anomalies, renal anomalies, and limb anomalies) association. *The Journal of Pediatrics*, *164*(3), 451–457.e451. https://doi.org/10.1016/j.jpeds.2013.10.086

van den Hondel, D., Wijers, C. H. W., van Bever, Y., de Klein, A., Marcelis, C. L. M., de Blaauw, I., … Ijsselstijn, H. (2016). Patients with anorectal malformation and upper limb anomalies: Genetic evaluation is warranted. *European Journal of Pediatrics*, *175*, 489–497. https://doi.org/10.1007/s00431-015-2655-9

Wisniewska, M., Karlberg, T., Lehtiö, L., Johansson, I., Kotenyova, T., Moche, M., & Schüler, H. (2010). Crystal structures of the ATPase domains of four human Hsp70 isoforms: HSPA1L/Hsp70-hom, HSPA2/Hsp70-2, HSPA6/Hsp70B', and HSPA5/BiP/GRP78. *PLoS One*, *5*(1), e8625. https://doi.org/10.1371/journal.pone.0008625

Zhang, R., Thiele, H., Bartmann, P., Hilger, A. C., Berg, C., Herberg, U., … Reutter, H. (2016). Whole-exome sequencing in nine monozygotic discordant twins. *Twin Research and Human Genetics Impact*, *19*(1), 60–65. https://doi.org/10.1017/thg.2015.93

Zhu, Y., Zhou, H., Zhu, Y., Wan, X., Zhu, J., & Zhang, T. (2012). Gene expression of Hsp70 , Hsp90 , and Hsp110 families in normal and abnormal embryonic development of mouse forelimbs. *Drug and Chemical Toxicology*, *35*(4), 432–444. https://doi.org/10.3109/01480545.2011.640683

How to cite this article: Kause F, Zhang R, Ludwig M, et al. *HSPA6*: A new autosomal recessive candidate gene for the VATER/VACTERL malformation spectrum. *Birth Defects Research*. 2019;1–7. https://doi.org/10.1002/bdr2.1493

MOLECULAR MEDICINE REPORTS 17: 3200-3205, 2018

Whole exome sequencing identifies a mutation in *EYA1* and *GLI3* in a patient with branchio-otic syndrome and esophageal atresia: Coincidence or a digenic mode of inheritance?

FRANZISKA KAUSE[1], HEIKO REUTTER[1,2], FLORIAN MARSCH[1], HOLGER THIELE[3], JANINE ALTMÜLLER[3,4], MICHAEL LUDWIG[5] and RONG ZHANG[1,6]

[1]Institute of Human Genetics, University Hospital of Bonn; [2]Department of Neonatology and Pediatric Intensive Care, Children's Hospital, University Hospital of Bonn, D-53127 Bonn; [3]Cologne Center for Genomics; [4]Institute of Human Genetics, University of Cologne, D-50931 Cologne; [5]Department of Clinical Chemistry and Clinical Pharmacology, University Hospital of Bonn; [6]Department of Genomics, Life and Brain Center, D-53127 Bonn, Germany

Received August 15, 2017; Accepted November 9, 2017

DOI: 10.3892/mmr.2017.8196

Abstract. Branchio-otic (BO) syndrome is a clinically and genetically heterogeneous disorder that presents with variable branchial arch and otic anomalies. Dominant mutations in the human homologues of the *Drosophila eyes absent* (*EYA1*) gene, and the *Drosophila sine oculis* homeobox 1 and 5 (*SIX1* and *SIX5*, respectively) genes have been causally associated with BO syndrome. Esophageal atresia (EA), with or without tracheo-esophageal fistula (TEF), is the most common type of malformation of the upper digestive tract. To date, its causes are poorly understood. The present study investigated a family with three affected members who all presented with classic BO associated symptoms. Notably, the index patient also presented with the most common EA/TEF subtype type 3b. Whole exome sequencing (WES) was performed in the index patient, and prioritized genetic variants and their segregation in the family were analyzed by Sanger sequencing. WES demonstrated a known disease-causing heterozygous *EYA1* splice variant in the patient, as well as his sister and mother; all of whom were affected with BO syndrome. A further GLI family zinc finger 3 (*GLI3*) splice variant of unknown significance, inherited from the unaffected father, was also detected in the index patient. *EYA1* and *GLI3* are involved in the Sonic Hedgehog transcriptional network and *GLI3* seems to be involved in human foregut malformations. Therefore, one may hypothesize a digenic inheritance model involving *EYA1* and *GLI3*, where the effect of the *GLI3* variant observed here only emerges in the background of the *EYA1* defect.

Correspondence to: Mrs. Rong Zhang, Institute of Human Genetics, University Hospital of Bonn, Sigmund-Freud-Str. 25, D-53127 Bonn, Germany
E-mail: rongzhang@uni-bonn.de

Key words: branchio-otic syndrome, esophageal atresia, *Drosophila eyes absent*, GLI family zinc finger 3, whole exome sequencing

Introduction

The branchio-otic (BO) syndrome is characterized by branchial arch and otic anomalies. It presents heterogeneously, both clinically and genetically, and manifests with reduced penetrance and variable expressivity (1). BO syndrome is a rare autosomal-dominant disorder with a birth prevalence of about 1:40,000 (1). The first identified causative gene was the human homologue of the *Drosophila eyes absent* gene, *EYA1* (2). Vincent *et al* (3) demonstrated that BOR (branchio-oto-renal syndrome 1, BOR1; OMIM #113650) and BOS (branchio-otic syndrome 1, BOS1; OMIM #602588) are allelic disorders. Subsequently, mutations in the two human homologues of the *Drosophila sine oculis* homeobox 1 and 5 genes (*SIX1*, *SIX5*) have been detected (4,5). To date, defects of *SIX5* have been exclusively found in patients who additionally presented with congenital renal anomalies, whereas *SIX1* mutations have been found in patients with the classic BO phenotype. Evidence for further genetic heterogeneity of BO syndrome was provided by Kumar *et al*, who linked an additional form (BOS2; OMIM %120502) to a region on chromosome 1q31 (6).

Esophageal atresia (EA) with or without tracheo-esophageal fistula (TEF) are the most common malformations of the upper digestive tract. EA/TEF comprises five anatomical subtypes and these are classified on the basis of the location and the type of anastomosis that exists between the trachea and the esophagus (7). The birth prevalence of EA/TEF has been reported with 1 in 3,000 live births (8). Approximately 50% of affected individuals show an isolated phenotype, while the remaining patients present EA/TEF in combination with other congenital malformations, e.g., cardiac or renal anomalies (9). Furthermore, EA/TEF have been observed in over 50 distinct genetic syndromes, associations and sequences (9). The likely causes of EA/TEF are heterogeneous and, to date, remain poorly understood. However, previous study has implicated several developmental genes with emphasis on effectors of the Sonic Hedgehog (SHH) signaling pathway [*SHH*, GLI family zinc finger 1 *(GLI1)*, *GLI2*, *GLI3*] in mouse

models (10). In this context, Motoyama *et al* (10) found that in *Gli2*$^{-/-}$ mice, a reduction of 50% in the gene dosage of *Gli3* in a *Gli2*$^{-/-}$ background resulted in EA/TEF and a severe lung phenotype, suggestive of a possible digenic inheritance model.

In the present study, we investigated a family with three affected members who all presented with classic BO-associated symptoms. Interestingly, the index patient also showed the most common EA/TEF subtype type 3b according to Vogt (7).

Materials and methods

Subjects. Blood samples were collected from all family members of the index patient and a further 18 patients with EA/TEF and BO syndrome-associated anomalies, such as hearing loss or malformation of the ears. Written informed consent was obtained from all participants or from their proxies in the case of legal minors. The study was approved by the ethics committee of the Medical Faculty of the University of Bonn and was conducted in accordance with the principles of the Declaration of Helsinki.

Whole exome sequencing (WES) and data analysis. Blood samples were obtained from the family under study and isolation of genomic DNA from blood was carried out using a Chemagic Magnetic Separation Module I (Chemagen, Baesweiler, Germany).

Mutation analysis was performed on our patient by WES (enrichment kit: Nimble Gene SeqCap ES Human Exome Library 2.0) with the Genome Analyzer II (Illumina). Read alignment and detection of variants was done with genome analyzing software (Varbank; www.varbank.ccg.uni-koeln.de/). In particular, we filtered for high quality (coverage of more than six reads, a minimum quality score of 10, VQSLOD greater than -8) and rare (allele frequency <0.5%) autosomal variants in *EAY1*, *SIX1* and *EAY1-SIX1* pathway-related genes. In order to exclude pipeline specific artifacts, we also filtered against an in-house epilepsy cohort (n=511, AF <2%) of variations, which were created with the same analysis pipeline. The filter conditions were set to be more sensitive following manual inspections of aligned reads.

Variation analysis. Variations identified by WES were amplified from genomic DNA by polymerase chain reaction (PCR) and automated sequence analysis was carried out using standard procedures. In brief, primers were directed to all observed variations and the resultant PCR products were subjected to direct automated BigDye terminator sequencing (3130XL Genetic Analyzer; Applied Biosystems; Thermo Fisher Scientific, Inc., Waltham, MA, USA). Both strands from each amplicon were sequenced and segregation of the variations in the family was investigated by sequencing the respective PCR product in all members. Primer sequences for all gene variants under investigation are available upon request.

Data from the observed allele frequencies harboring the variants were obtained from the ExAc database (exac.broadinstitute.org). Interpretation of identified missense variants was carried out with the following prediction programs: MutPred (www.mutpred1.mutdb.org), Polyphen-2 (www.genetics.bwh.harvard.edu/pph2/), HumVar (included in Polyphen-2), SIFT (sift.jcvi.org) and PROVEAN (included in SIFT). The *GLI3* splice variant was analyzed according to Shapiro and Senapathy (11) and Human Splicing Finder 3.0 (12).

Results

Clinical observations. The investigated family has three affected members who all presented with classic BO-associated symptoms (Table I and Fig. 1). Interestingly, the index patient (II.3) presented with branchial anomalies (bilateral branchial cleft fistulas and preauricular pits) and the most common EA/TEF subtype type 3b according to Vogt (7). The sister (II.2) and the mother (I.2) of the patient also presented with BO syndrome-associated symptoms (hearing loss or impairment, ear and neck fistulas). His elder brother (II.1) had a preauricular tag. The father showed no anomalies (Fig. 1). To the best of our knowledge, this is the first report on the concurrence of BO syndrome and EA/TEF to date.

WES and segregation of identified variants. In the context of the index patient reported here, Eisner *et al* (13) were recently able to show that several of the EA/TEF-associated SHH pathway genes *GLI1, GLI2,* and *GLI3* interact with the BO syndrome-associated *EYA1-SIX1* pathway genes. Hence, we performed whole-exome sequencing (WES) in the index patient (i) to identify disease causing variants in *EYA1-SIX1* pathway genes (ii) and to identify variants in EA/TEF-associated SHH pathway genes (13). Mutation analysis was performed on our patient with WES and the applied filtering identified more than 50 variants (data not shown). From these, one obvious genetic variant explains most of the congenital anomalies seen in the family. An *EYA1* mutation (c.966+5G>A, according to ENSEMBL transcript ENST00000340726, with the A of the start methionine as no. 1) was present in the donor splice site of exon 10 in the index patient. Sanger sequencing confirmed the mutation in the patient as well as two other affected family members (sister: II.2, and the mother, I.2; Fig. 1 and Table I). This mutation is known to cause exon skipping with a premature termination codon in the resultant mRNA (14).

Our second analysis of the index patient's WES dataset focused on candidate variants with an allele frequency of <0.01 in SHH signaling pathway genes with special emphasis on *GLI1, GLI2, GLI3*, *SUFU*, *NRP1*, *NRP2*, and *SMO*. In this context, we detected additional heterozygous variants in *GLI1* (p.Thr176Met), *GLI3* (splice variant c.1028+3A>G, according to ENSEMBL transcript ENST00000395025, with the A of the start methionine as no.1), *NRP1* (p.Asp601Asn) and *SMO* (p.Arg168His) (Table II). Apart from the four variants in *GLI1*, *GLI3*, *NRP1* and *SMO*, WES did not detect any further variations that might be attributable to EA/TEF in our patient. Sanger sequencing confirmed all four variants in the index patient (Fig. 1). Two of the four variants in *GLI1* and *SMO* were transmitted from the *EYA1* carrying mother and the other two variants in *GLI3* and *NRP1* were transmitted from the healthy father (Fig. 1). Since the mother did not present with EA/TEF we excluded the two variants in *GLI1* and *SMO* as EA/TEF disease causing. As the variant in *NRP1* is located in a region of low conservation (Table II), it was also excluded.

Table I. Phenotypic features identified in patients with the *Drosophila eyes absent* c.966+5G>A mutation.

Author, year	Patient	Hearing loss	Ear anomalies	Branchial anomalies	Renal anomalies	Other features	(Refs.)
Kause *et al*	I.2	Unilateral inner ear (unspecified)	Middle ear	Unilateral fistula (ear)	-	-	Present study
Kause *et al*	II.2	-	-	Bilateral fistula (ear), unilateral fistula (neck)	-	-	Present study
Kause *et al*	II.3	-	-	Bilateral fistula (ear), bilateral fistula (neck)	-	Esophageal atresia (Vogt 3b)	Present study
Stockley *et al*, 2009	8	Mild	-	Not specified fistula and cyst, bilateral preauricular pit	URA	-	(14)[a]
Stockley *et al*, 2009	9	Yes, unspecified	-	n/a	URA	-	(14)[a]
Stockley *et al*, 2009	10	Mild-to-moderate (mixed)	Cup shaped ears, posteriorly rotated	Not specified fistula and cyst, unilateral preauricular pit	URA, VUR	-	(14)[a]
Krug *et al*, 2011	1,291	-	-	Yes (unspecified)	-	Bilateral cataract	(15)[a]
Song *et al*, 2013	7	Bilateral (mixed, unspecified)	Cochlear hypoplasia (bi), dilated vestibule (bi), enlarged vestibular aqueduct (bi); middle ear: Ossicular anomaly (bi) and deviated facial nerve (bi); enlarged endolymphatic sac (l) and duct (bi)	-	n/a	-	(16)[b]
Bekheirnia *et al*, 2017	Family 3	-	-	-	VUR, multicystic dysplastic kidney	-	(17)[a]

No phenotypic findings were given for two additional families reported by Stockley *et al* (14). [a]Mutation initially termed c.867G>A in this paper; [b]mutation initially termed c.699+5G>A in this paper; n/a, not available; VUR, vesico-ureteric reflux; URA, unilateral renal agenesis; bi, bilateral; l, left.

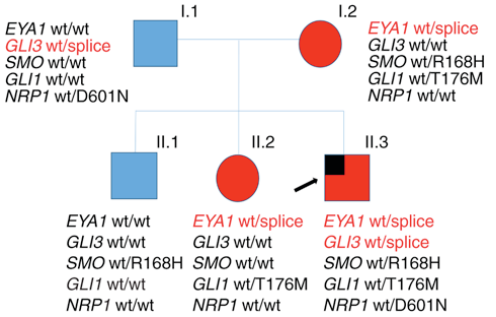

Figure 1. Pedigree of the family with BO syndrome. The index patient, also presenting with esophageal atresia, is marked by an arrow. The presence/absence of gene variants detected by whole-exome sequencing is indicated. Members affected with BO are shown in red, while unaffected members are shown in blue; males and females are indicated by squares and circles, respectively. BO, branchio-otic; wt, wild type; EYA1, *Drosophila eyes absent;* GLI, GLI family zinc finger; SMO, smoothened, frizzled class receptor; NRP1, neuropilin 1.

The remaining *GLI3* splice site variation, c.1028+3A>G, is an extremely rare variant (rs368499795), observed only once in the ExAc database (n=121,314 alleles). According to Shapiro and Senapathy (11), the A-to-G substitution slightly reduces the consensus value (CV) for splice site recognition from a CV of 0.887 for the wildtype sequence to a CV of 0.854 for the mutant one. As Human Splicing Finder 3.0 (12) also predicts this variation as most probably affecting splicing, these data imply that this *GLI3* variant interferes to a certain extent with correct mRNA processing.

To elucidate a more common involvement of EYA1 in the etiology of EA/TEF, we screened a further 18 patients with EA/TEF and BO syndrome-associated anomalies, such as hearing loss or malformation of the ears, for variants in *EYA1*. Sanger sequencing revealed 15 intronic and exonic common SNPs (allele frequencies all >0.08) and three further intronic variants with no influence on a splice site or a branch point (data not shown).

Discussion

The initial objective of the present study was to identify a genetic etiology of BO syndrome and EA/TEF in the index patient. Initially, WES demonstrated a heterozygous splice mutation in *EYA1*. To date, this c.966+5G>A mutation has been reported in nine other unrelated patients (Table I) (14-17), where it caused a pleiotropic spectrum of features. Stockley *et al* (14) reported the c.966+5G>A mutation in three BO syndrome patients, who each presented with the most severe renal phenotype in their cohort. However, it was associated without branchial and renal anomalies in a patient reported by Song *et al* (16), and only with branchial anomalies and congenital cataract in another patient (15). Most recently, Bekheirnia *et al* (17) detected the c.966+5G>A mutation in a patient solely affected with a renal phenotype, i.e., vesicoureteral reflux and multicystic dysplastic kidney. In the patient's family, the *EYA1* mutation caused branchial anomalies in the index patient (II.3) and all other affected subjects (I.2, II.2) as well as additional unilateral

Table II. Gene-prediction of the exonic variants with an amino-acid substitution and their conservation status.

Gene	Variation	Substitution	Mm	Dr	Gg	Xt	Polyphen	SIFT	MutPred (probability of deleterious mutation)	Variation frequency
GLI1	c.527C>T	T176M	T	T	T	T	Probably damaging	Damaging	0.290	rs755035040 (5.912x10^{-5})
GLI3	c.1028+3A>G	-	-	-	-	-	n/a	n/a	n/a	rs368499795 (8.24x10^{-6})
NRP1	c.1801G>A	D601N	D	-	D	A	Possibly damaging	Damaging	0.326	rs145594886 (4.97x10^{-5})
SMO	c.503G>A	R168H	R	K	K	K	Possibly damaging	Damaging	0.524	rs61746143 (0.009458)

Variation frequency was determined using Exome Aggregation Consortium (exac.broadinstitute.org). Mm, *Mus musculus*; Dr, *Danio rerio;* Gg, *Gallus gallus*; Xt, *Xenopus tropicalis*; n/a, not applicable as prediction programs do not score splice variants, however, Human Splicing Finder 3.0 (12) predicts that it most probably affects splicing; GLI, GLI family zinc finger; SMO, smoothened, frizzled class receptor; NRP1, neuropilin 1; SIFT, scale-invariant feature transform.

hearing loss in the mother (I.2). The older brother (II.1) of the index patient only presented with unilateral preauricular tag, a common benign congenital malformation of the external ear (18) possibly attributable to BO syndrome. Consequently, he was negative for the *EYA1* mutation. In conclusion, the detected *EYA1* mutation should explain all of the BO features observed in the index patient and the other family members.

Our second analysis of the index patient's WES dataset focused on candidate variants with an allele frequency of <0.01 in SHH signaling pathway genes. Evaluation of prioritized genes revealed the presence of an additional potential pathogenic *GLI3* splice variant (c.1028+3A>G) in the index case. Heterozygous mutations in *GLI3* are a most likely cause of Greig cephalopolysyndactyly syndrome (GCPS; OMIM #175700) and Pallister-Hall syndrome (PHS; OMIM #146510), both inherited as an autosomal dominant trait (19,20). Both disorders manifest polyaxial polydactyly with other overlapping features. However, neither a literature review nor the reviews of 174 GCPS/PHS patients, provided by Johnston *et al* (19,20), revealed the presence of our *GLI3* splice variant or EA/TEF in these patients. Yet, Yang *et al* (21) reported a *de novo* missense *GLI3* variant (p.M111T) in a patient with EA with hemivertebrae, resembling the phenotypic spectrum in murine models as reported by Motoyama *et al* (10).

Human Splicing Finder 3.0 (12), predicted the consequence of the c.1028+3A>G variant as most probably affecting splicing. However, according to Shapiro and Senapathy (11), the A-to-G substitution only slightly reduces the CV for splice site recognition, suggesting formation of a relevant amount of normally spliced mRNA, thereby avoiding GLI3 functional haploinsufficiency. This would explain the absence of typical phenotypic features caused by autosomal dominant *GLI3* mutations, as observed in patients with Pallister-Hall syndrome, Greig cephalopolysyndactyly syndrome or different forms of polydactyly (22). However, a small decrease in the formation of correct *GLI3* transcripts may interfere with the fine-tuning of the *Eya1-Six1*-SHH pathway. In mutant mice lungs, Lu *et al* (23) have shown that *Six1* and *Eya1* act together to regulate SHH/*Gli3* signaling activity. Lewandowski and coworkers reported that more than 40 GLI target genes in the mammalian limb bud are predominantly regulated by *GLI3*, but show a different spatiotemporal requirement for SHH signaling (24). Moreover, it has been reported that in murine peri-cloacal mesenchyme, *Six1* and *Eya1* functionally interact with the SHH pathway and that both these transcripts are down regulated in SHH mutants (25). Based on these observations, and since segregation analysis revealed the inheritance of the *GLI3* splice variant from the unaffected father, one may speculate about a digenic inheritance model involving *EYA1* and *GLI3*, where the effect of the *GLI3* variant emerges only in the background of the *EYA1* defect.

However, the recent work of Eisner *et al* (13), who described *Eya1* and *Six1* as key components of the Shh transcriptional network with *Eya1* and *Six1* as co-regulators of *Gli* transcriptional activators during normal organ development, and several other findings are suggestive of a direct involvement of *EYA1*/*Eya1* in esophageal development in vertebrates. In mice, *Eya1* has been shown to play a critical role in epithelial, mesenchymal and vascular morphogenesis of the embryonic lung as an upstream coordinator of SHH fibroblast growth factor 10 (Fgf10) signaling (26). It has been shown that the foregut epithelium gives rise to the esophagus, trachea, lungs, thyroid, stomach, liver, pancreas, and hepatobiliary system and there is experimental evidence that they are derived from a common progenitor cell population in the ventral foregut (27). Hence, in case of *EYA1* haploinsufficiency, impairment of this SHH-FGF10 cascade might also interfere with correct esophageal development. In zebra fish, requirement of Shh and *Fgf10* for esophageal morphogenesis has been reported (28) and similarly, disruption of the *Fgf10* gene during the critical period of separation of the trachea and esophagus caused tracheo-esophageal malformations in a mouse model (29). Moreover, it has been shown in mice that the Shh-Fgf10 cascade controls the patterning of the tracheal cartilage rings (30), and that defective Shh and Fgf signaling plays a role in the pathogenesis of EA/TEF (31). Here, the coexistence of the *EYA1* mutation and the additional variant in trans in *GLI3* of our patient is suggestive of a possible digenic mode of inheritance and might explain the co-occurrence of BO syndrome and EA/TEF in our patient. Screening of 18 EA/TEF patients with BO syndrome-associated phenotypic features did not reveal any additional *EYA1* mutation. While investigations of larger EA/TEF cohorts with BO syndrome-associated phenotypic features are warranted, our present approach to elucidate the coincidence of BO syndrome and EA/TEF in the index patient did not imply trio-based WES analysis. Hence, we cannot exclude any other possibly disease causing *de novo* mutations as the cause of EA/TEF in our patient.

Acknowledgements

We thank the family for their invaluable help. Pia Uerdingen is acknowledged for excellent assistance. F.K. was supported by the BONFOR program of the University of Bonn (grant no. O-149.0096). H.R. was supported by a grant from the Else Kröner-Fresenius-Stiftung (EKFS; grant no. 2014_A14) and by two grants from the German Research Foundation (Deutsche Forschungsgemeinschaft, DFG; grant nos. RE 1723/1-1 and RE 1723/2-1). M.L was supported by a grant from the German Research Foundation (DFG; grant no. LU 731/3-1).

References

1. Fraser FC, Sproude JR and Halal F: Frequency of the branchio-oto-renal (BOR) syndrome in children with profound hearing loss. Am J Med Genet 7: 341-349, 1980.
2. Abdelhak S, Kalatzis V, Heilig R, Compain S, Samson D, Vincent C, Weil D, Cruaud C, Sahly I, Leibovici M, *et al*: A human homologue of the *Drosophila eyes absent* gene underlies Branchio-Oto-Renal (BOR) syndrome and identifies a novel gene family. Nat Genet 15: 157-164, 1997.
3. Vincent C, Kalatzis V, Abdelhak S, Chaib H, Compain S, Helias J, Vaneecloo FM and Petit C: BOR and BO syndromes are allelic defects of EYA1. Eur J Hum Genet 5: 242-246, 1997.
4. Ruf RG, Xu PX, Silvius D, Otto EA, Beekmann F, Muerb UT, Kumar S, Neuhaus TJ, Kemper MJ, Raymond RM Jr, *et al*: SIX1 mutations cause branchio-oto-renal syndrome by disruption of EYA1-SIX1-DNA complexes. Proc Natl Acad Sci USA 101: 8090-8095, 2004.
5. Hoskins BE, Kramer CH, Silvius D, Zou D, Raymond RM, Orten DJ, Kimberling WJ, Smith RJ, Weil D, Petit C, *et al*: Transcription factor SIX5 is mutated in patients with branchio-oto-renal syndrome. Am J Hum Genet 80: 800-804, 2007.

6. Kumar S, Deffenbacher K, Marres HA, Cremers CW and Kimberling WJ: Genomewide search and genetic localization of a second gene associated with autosomal dominant branchio-oto-renal syndrome: Clinical and genetic implications. Am J Hum Genet 66: 1715-1720, 2000.
7. Vogt EC: Congenital esophageal atresia. Am J Roentgenol 22: 463-465, 1929.
8. Depaepe A, Dolk H and Lechat MF: The epidemiology of tracheo-esophageal fistula and oesophageal atresia in Europe. EUROCAT Working Group. Arch Dis Child 68: 743-748, 1993.
9. De Jong EM, Douben H, Eussen BH, Felix JF, Wessels MW, Poddighe PJ, Nikkels PG, de Krijer RR, Tibboel D and de Klein A: 5q11.2 deletion in a patient with tracheal agenesis. Eur J Hum Genet 18: 1265-1268, 2010.
10. Motoyama J, Liu J, Mo R, Ding Q, Post M and Hui CC: Essential function of Gli2 and Gli3 in the formation of lung, trachea and oesophagus. Nat Genet 20: 54-57, 1998.
11. Shapiro MB and Senapathy P: RNA splice junctions of different classes of eukaryotes: Sequence statistics and functional implications in gene expression. Nucleic Acids Res 15: 7155-7174, 1987.
12. Desmet FO, Hamroun D, Lalande M and Collod-Béroud G, Claustres M and Béroud C: Human splicing finder: An online bioinformatics tool to predict splicing signals. Nucleic Acids Res 37: e67, 2009.
13. Eisner A, Pazyra-Murphy MF, Durresi E, Zhou P, Zhao X, Chadwick EC, Xu PX, Hillman RT, Scott MP, Greenberg ME and Segal RA: The eya1 phosphatase promotes shh signaling during hindbrain development and oncogenesis. Dev Cell 33: 22-35, 2015.
14. Stockley TL, Mendoza-Londono R, Propst EJ, Sodhi S, Dupuis L and Papsin BC: A recurrent EYA1 mutation causing alternative RNA splicing in branchio-oto-renal syndrome: Implications for molecular diagnostics and disease mechanism. Am J Med Genet A 149A: 322-327, 2009.
15. Krug P, Moriniére V, Marlin S, Koubi V, Gabriel HD, Colin E, Bonneau D, Salomon R, Antignac C and Heidet L: Mutation screening of the EYA1, SIX1 and SIX5 genes in a large cohort of patients harboring branchio-oto-renal syndrome calls into question the pathogenic role of SIX5 mutations. Hum Mutat 32: 183-190, 2011.
16. Song MH, Kwon TJ, Kim HR, Jeon JH, Baek JI, Lee WS, Kim UK and Choi JY: Mutational analysis of EYA1, SIX1 and SIX5 genes and strategies for management of hearing loss in patients with BOR/BO syndrome. PLoS One 8: e67236, 2013.
17. Bekheirnia MR, Bekheirnia N, Bainbridge MN, Gu S, Coban Akdemir ZH, Gambin T, Janzen NK, Jhangiani SN, Muzny DM, Michael M, *et al*: Whole-exome sequencing in the molecular diagnosis of individuals with congenital anomalies of the kidney and urinary tract and identification of a new causative gene. Genet Med 19: 412-420, 2017.
18. Firat Y, Şireci Ş, Yakinci C, Akarçay M, Karakaş HM, Firat AK, Kizilay A and Selimoğlu E: Isolated preauricular pits and tags: Is it necessary to investigate renal abnormalities and hearing impairment? Eur Arch Otorhinolaryngol 265: 1057-1060, 2008.
19. Johnston JJ, Olivos-Glander I, Killoran C, Elson E, Turner JT, Peters KF, Abbott MH, Aughton DJ, Aylsworth AS, Bamshad MJ, *et al*: Molecular and clinical analyses of greig cephalopolysyndactyly and pallister-hall syndromes: Robust phenotype prediction from the type and position of GLI3 mutations. Am J Hum Genet 76: 609-622, 2005.
20. Johnston JJ, Sapp JC, Turner JT, Amor D, Aftimos S, Aleck KA, Bocian M, Bodurtha JN, Cox GF, Curry CJ, *et al*: Molecular analysis expands the spectrum of phenotypes associated with GLI3 mutations. Hum Mutat 31: 1142-1154, 2010.
21. Yang L, Shen C, Mei M, Zhan G, Zhao Y, Wang H, Huang G, Qiu Z, Lu W and Zhou W: De novo GLI3 mutation in esophageal atresia: Reproducing the phenotypic spectrum of Gli3 defects in murine models. Biochim Biophys Acta 1842: 1755-1761, 2014.
22. Al-Qattan MM, Shamseldin HE, Salih MA and Alkuraya FS: GLI3-related polydactyly: A review. Clin Genet, 2017.
23. Lu K, Reddy R, Berika M, Warburton D and El-Hashash AH: Abrogation of Eya1/Six1 disrupts the saccular phase of lung morphogenesis and causes remodeling. Dev Biol 382: 110-123, 2013.
24. Lewandowski JP, Du F, Zhang S, Powell MB, Falkenstein KN, Ji H and Vokes SA: Spatiotemporal regulation of GLI target genes in the mammalian limb bud. Dev Biol 406: 92-103, 2015.
25. Wang C, Gargollo P, Guo C, Tang T, Mingrin G, Sun Y and Li X: Six1 and Eya1 are critical regulators of peri-cloacal mesenchyme progenitors during genitourinary tract development. Dev Biol 360: 186-194, 2011.
26. El-Hashash AH, Al Alam D, Turcatel G, Bellusci S and Warburton D: Eyes absent 1 (Eya1) is a critical coordinator of epithelial, mesenchymal and vascular morphogenesis in the mammalian lung. Dev Biol 350: 112-126, 2011.
27. Zaret KS: Genetic programming of liver and pancreas progenitors: Lessons for stem-cell differentiation. Nat Rev Genet 9: 329-340, 2008.
28. Korzh S, Winata CL, Zheng W, Yang S, Yin A, Ingham P, Korzh V and Gong Z: The interaction of epithelial Ihha and mesenchymal Fgf10 in zebrafish esophageal and swimbladder development. Dev Biol 359: 262-276, 2011.
29. Hajduk P, Murphy P and Puri P: Fgf10 gene expression is delayed in the embryonic lung mesenchyme in the adriamycin mouse model. Pediatr Surg Int 26: 23-27, 2010.
30. Sala FG, Del Moral PM, Tiozzo C, Al Alam D, Warburton D, Grikscheit T, Veltmaat JM and Bellusci S: FGF10 controls the patterning of the tracheal cartilage rings via Shh. Development 138: 273-282, 2011.
31. Spilde T, Bhatia A, Ostlie D, Marosky J, Holcomb G III, Snyder C and Gittes G: A role for sonic hedgehog signaling in the pathogenesis of human tracheoesophageal fistula. J Pediatr Surg 38: 465-468, 2003.

REPORT

CAKUT and Autonomic Dysfunction Caused by Acetylcholine Receptor Mutations

Nina Mann,[1,14] Franziska Kause,[1,14] Erik K. Henze,[2] Anant Gharpure,[3] Shirlee Shril,[1] Dervla M. Connaughton,[1] Makiko Nakayama,[1] Verena Klämbt,[1] Amar J. Majmundar,[1] Chen-Han W. Wu,[1] Caroline M. Kolvenbach,[1] Rufeng Dai,[1] Jing Chen,[1] Amelie T. van der Ven,[1] Hadas Ityel,[1] Madeleine J. Tooley,[4] Jameela A. Kari,[5] Lucy Bownass,[4] Sherif El Desoky,[5] Elisa De Franco,[6] Mohamed Shalaby,[5] Velibor Tasic,[7] Stuart B. Bauer,[8] Richard S. Lee,[8] Jonathan M. Beckel,[9] Weiqun Yu,[10] Shrikant M. Mane,[11] Richard P. Lifton,[11,12] Heiko Reutter,[13] Sian Ellard,[6] Ryan E. Hibbs,[3] Toshimitsu Kawate,[2] and Friedhelm Hildebrandt[1,*]

Congenital anomalies of the kidney and urinary tract (CAKUT) are the most common cause of chronic kidney disease in the first three decades of life, and *in utero* obstruction to urine flow is a frequent cause of secondary upper urinary tract malformations. Here, using whole-exome sequencing, we identified three different biallelic mutations in *CHRNA3*, which encodes the α3 subunit of the nicotinic acetylcholine receptor, in five affected individuals from three unrelated families with functional lower urinary tract obstruction and secondary CAKUT. Four individuals from two families have additional dysautonomic features, including impaired pupillary light reflexes. Functional studies *in vitro* demonstrated that the mutant nicotinic acetylcholine receptors were unable to generate current following stimulation with acetylcholine. Moreover, the truncating mutations p.Thr337Asnfs*81 and p.Ser340* led to impaired plasma membrane localization of CHRNA3. Although the importance of acetylcholine signaling in normal bladder function has been recognized, we demonstrate for the first time that mutations in *CHRNA3* can cause bladder dysfunction, urinary tract malformations, and dysautonomia. These data point to a pathophysiologic sequence by which monogenic mutations in genes that regulate bladder innervation may secondarily cause CAKUT.

Congenital anomalies of the kidney and urinary tract (CAKUT) represent up to 20%–30% of all prenatally detected anomalies and are the most common cause of chronic kidney disease in the first three decades of life.[1–3] The discovery of more than 40 monogenic causes of CAKUT in humans has led to the understanding that urogenital malformations often arise from defects in the signaling pathways that regulate nephrogenesis.[4–6] In addition, animal studies have demonstrated that intrauterine obstruction to urine flow can secondarily lead to CAKUT, although the genetic etiologies and molecular pathogenesis of these processes are not well understood.[7]

Nicotinic acetylcholine receptors (nAChR) are heteropentameric ligand-gated ion channels that are widely expressed in the nervous system and in certain non-neuronal tissues, such as the bladder urothelium.[8,9] Interestingly, mice lacking *Chrna3*, the gene encoding the α3 nAChR subunit, develop a prominent genitourinary phenotype, with reduced bladder contractility, megacystis, and recurrent urinary tract infections.[10] The α3 nAChR subunit mediates fast synaptic transmission in the parasympathetic, sympathetic, and enteric ganglia and plays a critical role in modulating normal bladder function.[11]

To date, only one gene involved in neuronal synaptic transmission, *CHRM3* (MIM: 118494), has been implicated in lower urinary tract obstruction in humans.[12] Here, we describe the discovery of biallelic mutations in *CHRNA3* in three families with CAKUT and additional extra-renal dysautonomic features.

Approval for human subject research was obtained from the Institutional Review Board at the respective institutions, and samples were obtained after written informed consent. The index case subject, B1717-21, is a young man who was born to consanguineous parents of Arabic descent and who presented in childhood with recurrent urinary tract infections. Renal ultrasound demonstrated bilateral hydronephrosis, a thickened bladder wall, and a large post-void residual (Figure 1A). Voiding cysturethrogram (VCUG) revealed bilateral grade 5 vesicoureteral reflux (VUR) without posterior urethral valves (not shown), and the affected individual was given a diagnosis of non-neurogenic neurogenic bladder. He developed progressive

[1]Department of Pediatrics, Boston Children's Hospital, Boston, MA 02115, USA; [2]Department of Molecular Medicine, Cornell University, Ithaca, NY 14853, USA; [3]Departments of Neuroscience and Biophysics, University of Texas Southwestern Medical Center, Dallas, TX 75390, USA; [4]Department of Clinical Genetics, St. Michael's Hospital, University Hospital's Bristol NHS Foundation Trust, Bristol BS2 8EG, UK; [5]Pediatric Nephrology Center of Excellence and Pediatric Department, Faculty of Medicine, King Abdulaziz University, Jeddah 21859, Kingdom of Saudi Arabia; [6]Institute of Biomedical and Clinical Science, University of Exeter Medical School, Exeter EX2 5DW, UK; [7]Medical Faculty Skopje, University Children's Hospital, Skopje 1000, Macedonia; [8]Department of Urology, Boston Children's Hospital, Boston, MA 02115, USA; [9]Department of Pharmacology and Chemical Biology, University of Pittsburgh, Pittsburgh, PA 15261, USA; [10]Division of Nephrology, Beth Israel Deaconess Medical Center, Boston, MA 02215, USA; [11]Department of Genetics, Yale University School of Medicine, New Haven, CT 06520, USA; [12]Laboratory of Human Genetics and Genomics, The Rockefeller University, New York, NY 10065, USA; [13]Institute of Human Genetics, University of Bonn, Bonn 53127, Germany Department of Neonatology and Pediatric Intensive Care, Children's Hospital, University of Bonn, Bonn 53127, Germany
[14]These authors contributed equally to this work
*Correspondence: friedhelm.hildebrandt@childrens.harvard.edu
https://doi.org/10.1016/j.ajhg.2019.10.004.

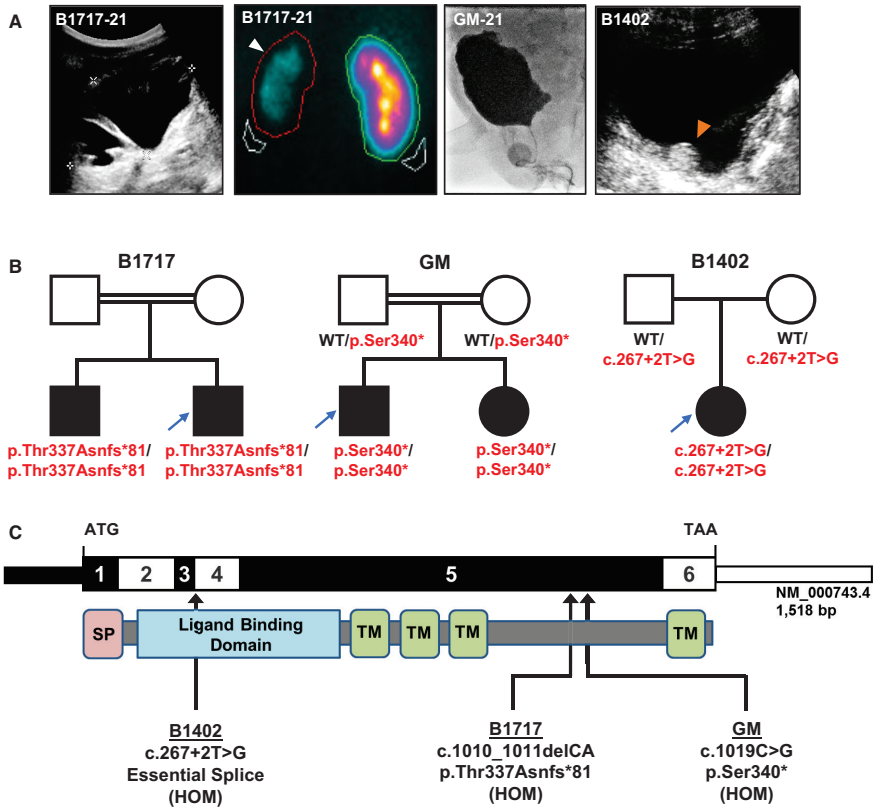

Figure 1. Identification of Biallelic *CHRNA3* Mutations in Three Families with CAKUT
(A) Renal and bladder imaging for affected individuals. The two left panels depict a renal ultrasound and DMSA (dimercaptosuccinic acid) scan from individual B1717-21. The renal ultrasound demonstrates severe left-sided hydronephrosis with cortical thinning, and DMSA scan shows reduced cortical uptake of the left kidney (arrow head). VCUG from individual GM-21 and bladder ultrasound from individual B1402 both demonstrate thickened and irregular bladder walls. The echogenic circular irregularity on the bladder ultrasound for B1402 (orange arrowhead) is an artifact from a STING procedure that was done after recurrent vesicoureteral reflux developed following bilateral ureteral reimplantation.
(B) Pedigrees for the three affected families. In the pedigrees, squares represent males and circles represent females. Open symbols represent unaffected individuals, and filled symbols represent affected individuals. Consanguineous unions are depicted as double horizontal lines. Probands (individuals -21 of each family) are denoted by blue arrows. WT, wild type.
(C) Exon and protein domain structure of *CHRNA3*. The exon structure is depicted in the upper bar, with positions of the start codon (ATG) and stop codon (TAA) indicated. The lower bar depicts the protein structure of CHRNA3, with an N-terminal signal peptide (pink), a large extracellular ligand-binding domain (blue), and four transmembrane helices (green). The three different mutations detected in three families are mapped to the exon and protein structures.

renal insufficiency, and by 19 years of age, a DMSA scan demonstrated a small, atrophic left kidney with 10% residual function (Figure 1A). He also presented to the ophthalmologist in adolescence for difficulty seeing in bright light and was found to have bilateral mydriasis with impaired pupillary constriction. Moreover, orthostatic hypotension was diagnosed on routine physical examination (Table 1). The proband's brother, B1717-22, was also noted to have an impaired pupillary light reflex. He additionally has a history of recurrent urinary tract infections, although renal ultrasound revealed normal-appearing kidneys and bladder (not shown).

We applied whole-exome sequencing (WES) and homozygosity mapping to individual B1717-21.[13,14] Mutation calling was performed in line with proposed guidelines by clinician-scientists who had knowledge of the clinical phenotypes and pedigree structure (Figure S1).[15] We identified a homozygous truncating mutation (GenBank: NM_000743.4; c.1010_1011delCA [p.Thr337Asnfs*81]) in exon 5 of the gene *CHRNA3* (Cholinergic Receptor

Table 1. Recessive Mutations Identified in *CHRNA3* in Three Families with CAKUT

Family	Ethnic Origin	Gender	Exon (Zygosity)	Nucleotide Change; Amino Acid Change (Segregation)[a]	gnomAD Allele Frequencies[b]	Genitourinary Manifestations	Dysautonomic Manifestations	Other[c]
B1402	Macedonian	female	intron 3 (hom)	c.267+2T>G (essential splice); (m. het; p. het)	0/1/246,220	bilat. VUR, grade IV recurrent VUR post ureteral reimplantation CKD (stage 2)	none	none
B1717-21	Arabic	male	exon 5 (hom)	c.1010_1011delCA (p.Thr337Asnfs*81); (ND)	NP	non-neurogenic neurogenic bladder bilat. VUR, grade V bilat. hydronephrosis atrophic left kidney CKD (stage 2)	impaired pupillary light reflex orthostatic hypotension	none
B1717-22	Arabic	male	exon 5 (hom)	c.1010_1011delCA (p.Thr337Asnfs*81); (ND)	NP	recurrent UTIs	impaired pupillary light reflex	none
GM-21	Pakistani	male	exon 5 (hom)	c.1019C>G (p.Ser340*); (m. het; p. het)	0/4/246,010	non-neurogenic neurogenic bladder left hydronephrosis right cystic kidney hypospadias	impaired pupillary light reflex flat CTG tracing *in utero*	hypertelorism broad nasal root intellectual disability 2q31.1-32.3 duplication (*de novo*)
GM-22	Pakistani	female	exon 5 (hom)	c.1019C>G (p.Ser340*); (m. het; p. het)	0/4/246,010	voiding dysfunction recurrent UTIs	impaired pupillary light reflex flat CTG tracing *in utero*	GERD, failure to thrive

Abbreviations: Bilat., bilateral; CKD, chronic kidney disease; CTG, cardiotocography; GERD, gastresophageal reflux; het, heterozygous; Hom, homozygous; m, maternal allele; ND, no data; NP, not present; p, paternal allele; UTI, urinary tract infection; VUR, vesicoureteral reflux.
[a]Segregation is listed as (maternal allele, paternal allele) when available. If parental DNA was not available, segregation is listed as ND.
[b]None of the identified *CHRNA3* mutations have been reported homozygously in gnomAD, which includes exome or genome sequencing data from 141,456 unrelated individuals.
[c]One affected individual was found to have additional genetic abnormalities that were thought to explain some of his extra-renal manifestations. GM-21 has a *de novo* 2q31.1–32.3 duplication which may explain his facial dysmorphisms and intellectual disability. This duplication was not shared by his sister, GM-22.

Nicotinic Alpha 3 Subunit), which encodes the α3 nAChR subunit. The same homozygous mutation was found in the proband's affected older brother, B1717-22 (Figure 1B, Table 1).

Through the use of the on-line tool, GeneMatcher,[16,17] we identified two siblings of Pakistani descent (GM-21 and GM-22) who also have biallelic mutations in *CHRNA3* (c.1019C>G [p.Ser340*]). GM-21 was diagnosed prenatally with hydronephrosis, and post-natal imaging revealed a dilated, cystic right kidney, left hydroureteronephrosis, and a thickened, trabeculated bladder wall (Figure 1A). He was diagnosed with non-neurogenic neurogenic bladder and was managed with clean intermittent catheterizations and subsequent vesicostomy. His younger sister, GM-22, had recurrent urinary tract infections, and VCUG demonstrated a large-capacity bladder with incomplete emptying (not shown). Ophthalmology examination for both children revealed constant miosis with pupils that did not dilate, and both siblings additionally had flat cardiotocography (CTG) tracings *in utero*. This was detected at 36 weeks gestational age in the older child, for which he underwent emergent cesarean section. A flat CTG tracing was noticed at 29 weeks gestational age for the younger sibling and persisted until she was delivered at full term.

We subsequently queried WES data in our cohort of 380 families with CAKUT and identified one additional affected individual with biallelic *CHRNA3* mutations. In individual B1402, who has bilateral VUR and hydronephrosis, we detected a homozygous essential splice site mutation (c.267+2T>G). Interestingly, this individual underwent ureteral reimplantation as a child but developed recurrence of her VUR, for which she underwent a STING procedure (Figure 1A). We did not detect any biallelic mutations in *CHRNA3* in a control cohort of 419 families with either nephrotic syndrome or nephronophthisis.

All three *CHRNA3* mutations were confirmed via Sanger sequencing (Figure S3). A summary of the clinical characteristics of the affected individuals and the mutations identified is provided in Table 1, and a schematic of the *CHRNA3* exon and protein structure with locations of the three mutations is depicted in Figure 1C. Both the p.Thr337Asnfs*81 and p.Ser340* variants are predicted to lead to premature termination of the protein prior to the fourth transmembrane helix (Figure 1C). As RNA was not available from the individual with the c.267+2T>G splice mutation, we used *in silico* prediction tools to determine the splicing effect. Because the c.267+2T>G change occurs at an obligatory splice site, we predict that this will lead to skipping of exon 3 and an in-frame deletion of 15 amino acids in the protein's extracellular ligand-binding domain. However, it should be noted that this may not recapitulate the splicing effect *in vivo*.

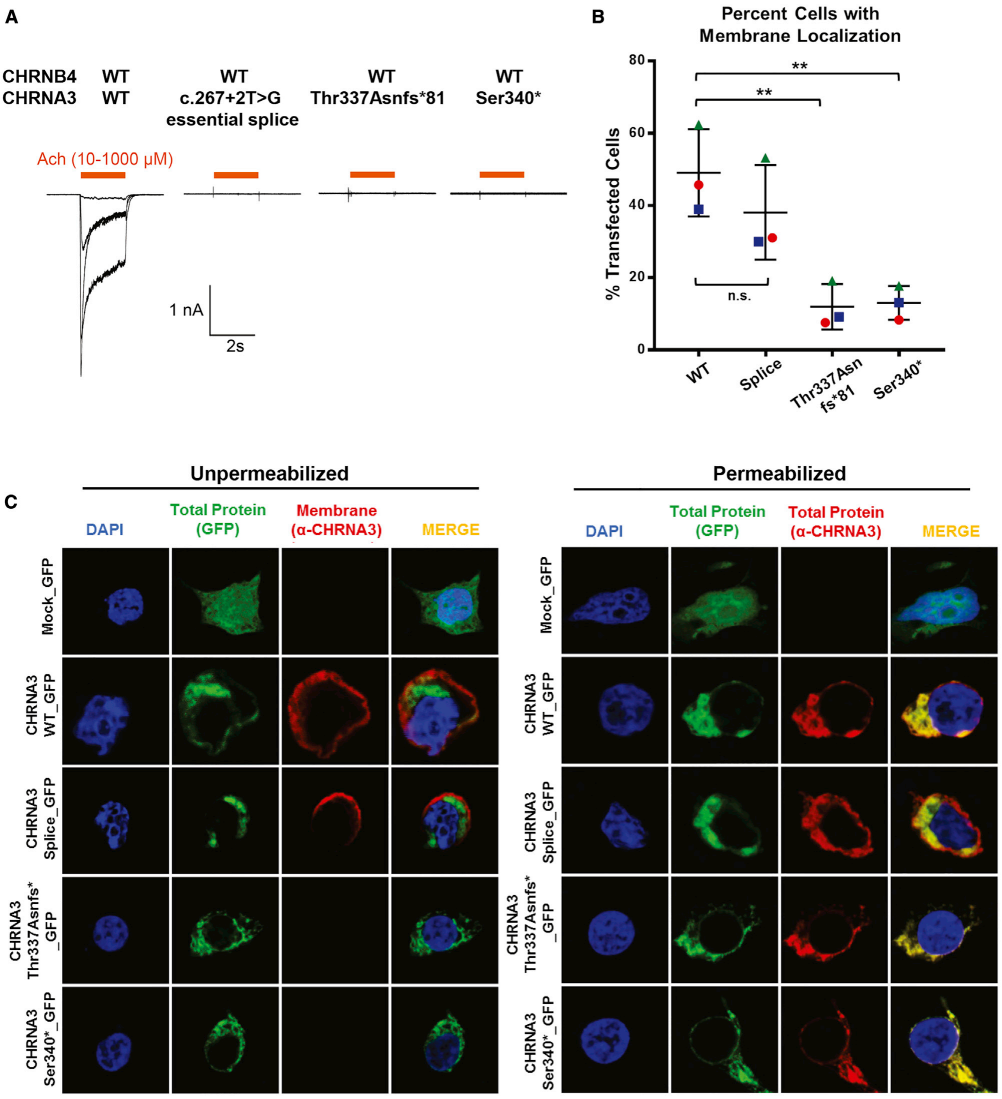

Figure 2. ***CHRNA3*** **Mutants Perturb α3β4 nAChR Function and Impair Plasma Membrane Trafficking**

(A) Whole-cell currents obtained from HEK293 cells overexpressing both wild-type and the indicated mutant α3β4 nicotinic acetylcholine receptors (nAChRs). Wild-type α3β4 nAChR generates a strong current after incubation with acetylcholine (n = 7). In contrast, the essential splice (n = 4), p.Thr337Asnfs*81 (n = 4), and p.Ser340* (n = 4) mutants were unable to generate any current.

(B) Membrane localization of α3 nAChR in HEK293 cells. Quantification of immunofluorescence images of HEK293 cells overexpressing either wild-type or mutant GFP-tagged CHRNA3. Graphs represent an average of three independent experiments. For each experiment, 100–150 transfected cells were evaluated for membrane staining. 49% of cells transfected with WT-CHRNA3 demonstrated membrane staining. In contrast, only 12%–13% of cells transfected with the p.Thr337Asnfs*81 and p.Ser340* mutants demonstrate membrane staining, respectively. The error bars represent SEM for three experiments. **p value < 0.01 when compared to wild type; n.s. not significant when compared to wild type.

(C) Representative immunofluorescence images depicting the cellular localization of overexpressed GFP-tagged wild-type and mutant α3 nAChRs in HEK293 cells. Unpermeabilized (left) and permeabilized (right) cells are stained with an anti-CHRNA3 antibody raised against the protein's extracellular N terminus. The green GFP signal demonstrates total transfected CHRNA3 protein, whereas in

(legend continued on next page)

In the two families in which homozygosity mapping was available, the *CHRNA3* mutations were all located within regions of homozygosity by descent (Figure S4). None of the three *CHRNA3* variants were present homozygously in the large population database, gnomAD (Table 1). Exome data for each proband from the three families were also analyzed for mutations in known CAKUT genes[5] and no causative variants were identified. However, individual GM-21 was noted to have a *de novo* 25.6 Mb duplication of chromosome 2q31.1–2q32.3 that was not shared by his affected sister. This is thought to contribute to his cognitive deficits, although further studies will be required for causality to be more definitively established.

In order to examine whether the identified mutations in *CHRNA3* affect receptor function, we performed electrophysiology and immunofluorescence studies in HEK293 cells. The α3 nAChR subunit is known to heteropentamerize with the β4 nAChR subunit,[18] and we first aimed to determine whether the *CHRNA3* mutations affect the ability of the α3β4 nAChR to induce current after stimulation with acetylcholine. Patch-clamping experiments were performed in HEK293 cells co-transfected with wild-type *CHRNB4* cDNA and either wild-type or mutant *CHRNA3* cDNA. Acetylcholine induced a dose-dependent inward current in cells overexpressing the wild-type α3β4 nAChR (Figure 2A). In contrast, no current was generated in cells expressing receptors composed of the splice site, p.Thr337Asnfs81*, or p.Ser340* mutant α3 subunits (Figure 2A). These data demonstrate complete loss of function for the essential splice and two truncating variants.

Because the two truncating mutations (p.Thr337Asnfs*81 and p.Ser340*) lead to premature termination of the CHRNA3 protein prior to the fourth transmembrane helix, we hypothesized that this would disrupt membrane trafficking of the mutant receptors. We expressed GFP-tagged wild-type and mutant *CHRNA3* cDNA in HEK293 cells and labeled unpermeabilized cells with an antibody to the extracellular N terminus of the α3 nAChR subunit, which is expected to bind only those proteins that are inserted into the plasma membrane (Figures 2B and 2C). We detected membrane localization of the wild-type α3 nAChR subunit in 49% of transfected cells. In contrast, only 12%–13% of transfected cells demonstrated membrane staining for the p.Thr337Asnfs*81 and p.Ser340* mutants, suggesting impaired membrane trafficking (Figure 2B). There is a trend toward reduced membrane localization for the essential splice site variant, but this did not reach statistical significance. Representative immunofluorescence images are depicted in Figure 2C. Permeabilized cells, in which both extracellular and intracellular labeling is established, were utilized as controls.

We here discovered by whole-exome sequencing three different homozygous loss-of-function mutations in *CHRNA3* in three families with CAKUT. We demonstrate that all three mutations attenuate the ability of the α3β4 nAChR to generate current after stimulation with acetylcholine. Additionally, the two truncating mutations, p.Thr337Asnfs* and p.Ser340*, impair receptor trafficking to the plasma membrane.

Micturition requires coordinated stimulation of the urinary bladder and urethral sphincters by the parasympathetic, sympathetic, and somatic nervous systems (Figure S5).[11] *CHRNA3* mediates fast synaptic transmission in the autonomic ganglia, and we predict that loss of *CHRNA3* may result in discoordinated detrusor and urethral function. *CHRNA3* is also expressed in the bladder urothelium and therefore may play additional roles in regulating bladder contraction beyond its known function in the autonomic ganglia.[9] Of interest, all three families in our cohort developed secondary upper urinary tract malformations, such as hydronephrosis and renal cysts, consistent with the notion that obstruction to urinary flow *in utero* can lead to abnormalities in renal development.[7,19,20] Indeed, individual B1402 underwent bilateral ureteral reimplantation, only to develop recurrent VUR and worsening hydronephrosis, likely because her underlying bladder dysfunction had not been recognized. We propose that disruption of *CHRNA3* can result in a pathophysiological sequence by which impaired neuronal innervation leads to bladder dysfunction, functional lower urinary tract obstruction, and subsequent upper urinary tract anomalies.

In addition to their renal manifestations, families B1717 and GM, in whom truncating *CHRNA3* mutations were found, have dysautonomic features, most notably an impaired pupillary light reflex. Compellingly, autoantibodies to the α3 nAChR subunit have been described to cause an autoimmune autonomic ganglionopathy in humans.[21] These individuals develop profound autonomic failure, with symptoms overlapping those found in families with truncating *CHRNA3* mutations, including bladder dysfunction, impaired pupillary light reflexes, and orthostatic hypotension.[21,22] Notably, individual B1402 does not have dysautonomic manifestations. This may be due to subtle findings that are not clinically manifest, or it may be the case that hypomorphic mutations lead to a milder phenotype. Identification of additional affected individuals with *CHRNA3* mutations may provide further insight into genotype-phenotype correlations.

unpermeabilized cells, the red signal (anti-CHRNA3) depicts protein localized to the plasma membrane. Wild-type CHRNA3 and the splice site mutant both demonstrate membrane localization. In contrast, there is no signal from the anti-CHRNA3 antibody for the protein truncating p.Thr337Asnfs* and p.Ser340* mutants, suggesting impaired membrane localization. In permeabilized cells, both the GFP signal (green) and antibody staining (red) demonstrate cytoplasmic localization of the p.Thr337Asnfs* and p.Ser340* mutant proteins.

The genitourinary and ocular phenotypes seen in families B1717 and GM are strikingly similar to that of the *Chrna3*$^{-/-}$ mice, which have megacystis, recurrent urinary tract infections, and persistent mydriasis.[10] Bladder strips from these animals fail to contract in response to nicotine, and neurons from the superior cervical ganglia do not generate current in response to acetylcholine, consistent with the notion that loss of *CHRNA3* results in impaired fast synaptic transmission within the autonomic ganglia.[10] It is interesting to note that there is variable expressivity among affected individuals with *CHRNA3* mutations. The two siblings in family B1717, who harbor the same *CHRNA3* p.Thr337Asnfs*87 truncating mutation, for example, exhibit a range of renal phenotypes, from only recurrent urinary tract infections to severe hydronephrosis, vesicoureteral reflux, and chronic kidney disease. This supports the notion that the renal disease manifesting in these individuals is the result of a pathophysiological sequence whereby impairment of bladder contraction results in secondary upper urinary tract malformations. The degree of renal impairment is likely a result of stochastic changes that occur *in utero*, and such variable expressivity is often seen in a variety of other monogenic diseases that cause CAKUT.[4,23]

To date, few monogenic causes of bladder dysfunction have been described in humans, including mutations in the genes *CHRM3* (MIM: 118494), *ACTG2* (MIM: 102545), *ACTA2* (MIM: 102620), *MYH11* (MIM: 160745), *MYLK* (MIM: 600922), *HPSE2* (MIM: 613469), and *LRIG2* (MIM: 608869).[12,24–30] These genes have been implicated in the regulation of smooth muscle actin contraction, neuronal patterning, and synaptic neuronal transmission (Figure S5), and mutations cause syndromes such as megacystis-microcolon-intestinal hypoperistalsis syndrome (MMIHS [MIM: 155310, 613834]) or urofacial syndrome (MIM: 236730, 615112). Interestingly, individuals with mutations in *CHRM3*, which encodes a muscarinic acetylcholine receptor, also present with persistent mydriasis.[12] The findings in our study provide additional evidence that disruption of the neural pathways regulating bladder function can be important genetic causes of both CAKUT and autonomic dysfunction in humans.

Our findings may point to important therapeutic implications. Current management for children with lower urinary obstruction involves surgical intervention to relieve anatomic obstruction and subsequent medical management of the sequelae from chronic kidney disease.[31] However, surgical techniques alone may not be successful for individuals in whom mutations in *CHRNA3* are identified, as was the case for individual B1402. The neuronal pathways regulating bladder contraction additionally provide tractable therapeutic targets that may be amenable to pharmacological intervention. In addition, early prenatal genetic diagnoses might eventually allow for pharmacological interventions *in utero*, which could prevent the development of renal dysgenesis. Further identification of novel genetic causes of urinary tract obstruction will provide additional strategies toward precision medicine.

Supplemental Data

Supplemental Data can be found online at https://doi.org/10.1016/j.ajhg.2019.10.004.

Acknowledgments

We thank the affected individuals and their families for their contributions to this study. We also would like to thank Michael Wangler, Arthur Beaudet, Reza Bekheirnia, William Newman, and Fowzan Alkuraya for helpful discussion. This research was supported by grants from the National Institutes of Health to F.H. (DK0668306). N.M. is supported by funding from the National Institutes of Health (grant T32-DK007726). F.K. is supported by funding from the Biomedical Education Program. D.M.C. is funded by the Health Research Board, Ireland (HPF-206-674), the International Pediatric Research Foundation Early Investigators' Exchange Program, and the Amgen Irish Nephrology Society Specialist Registrar Bursary. M.N. is supported by a grant from the Japan Society for the Promotion of Science. V.K. is supported by the Deutsche Forschungsgemeinschaft (403877094). A.J.M. is supported by funding from the National Institutes of Health (grant T32-DK007726), the 2017 Harvard Stem Cell Institute Fellowship Grant, and the 2018 Jared J. Grantham Research Fellowship from the American Society of Nephrology Ben J. Lipps Research Fellowship Program. C.-H.W.W. is supported by funding from the National Institutes of Health (grant T32-GM007748). R.S.L. is supported by funding from the National Institutes of Health (DK096238). S.E. is a Wellcome Senior Investigator. F.H. is also supported by the Begg Family Foundation. We also thank the Yale Center for Mendelian Genomics for whole-exome sequencing analysis (U54HG006504).

Declaration of Interests

F.H. is a cofounder and S.A.C. member and holds stocks in Goldfinch-Bio. All other authors declare that they have no competing financial interests.

Received: June 11, 2019
Accepted: October 9, 2019
Published: November 7, 2019

Web Resources

1000 Genomes Project, https://www.internationalgenome.org/1000-genomes-browsers
Clustal Omega, https://www.ebi.ac.uk/Tools/msa/clustalo/
Exome Aggregation Consortium (ExAC), http://exac.broadinstitute.org
GenBank, https://www.ncbi.nlm.nih.gov/genbank/
Genome Aggregation Database (gnomAD), http://gnomad.broadinstitute.org
MutationTaster, http://www.mutationtaster.org
NHLBI Exome Sequencing Project (ESP), https://evs.gs.washington.edu/EVS
Online Mendelian Inheritance in Man (OMIM), https://www.omim.org
PolyPhen2, http://genetics.bwh.harvard.edu/pph2

Sorting Intolerant From Tolerant (SIFT), http://sift.jcvi.org
UCSC Genome Browser, https://genome.ucsc.edu

References

1. Ingelfinger, J.R., Kalantar-Zadeh, K., Schaefer, F.; and World Kidney Day Steering Committee (2016). World Kidney Day 2016: Averting the legacy of kidney disease-focus on childhood. Pediatr. Nephrol. *31*, 343–348.
2. Calderon-Margalit, R., Golan, E., Twig, G., Leiba, A., Tzur, D., Afek, A., Skorecki, K., and Vivante, A. (2018). History of Childhood Kidney Disease and Risk of Adult End-Stage Renal Disease. N. Engl. J. Med. *378*, 428–438.
3. Queisser-Luft, A., Stolz, G., Wiesel, A., Schlaefer, K., and Spranger, J. (2002). Malformations in newborn: results based on 30,940 infants and fetuses from the Mainz congenital birth defect monitoring system (1990-1998). Arch. Gynecol. Obstet. *266*, 163–167.
4. van der Ven, A.T., Vivante, A., and Hildebrandt, F. (2018). Novel Insights into the Pathogenesis of Monogenic Congenital Anomalies of the Kidney and Urinary Tract. J. Am. Soc. Nephrol. *29*, 36–50.
5. van der Ven, A.T., Connaughton, D.M., Ityel, H., Mann, N., Nakayama, M., Chen, J., Vivante, A., Hwang, D.Y., Schulz, J., Braun, D.A., et al. (2018). Whole-Exome Sequencing Identifies Causative Mutations in Families with Congenital Anomalies of the Kidney and Urinary Tract. J. Am. Soc. Nephrol. *29*, 2348–2361.
6. Verbitsky, M., Westland, R., Perez, A., Kiryluk, K., Liu, Q., Krithivasan, P., Mitrotti, A., Fasel, D.A., Batourina, E., Sampson, M.G., et al. (2019). The copy number variation landscape of congenital anomalies of the kidney and urinary tract. Nat. Genet. *51*, 117–127.
7. Chevalier, R.L., Thornhill, B.A., Forbes, M.S., and Kiley, S.C. (2010). Mechanisms of renal injury and progression of renal disease in congenital obstructive nephropathy. Pediatr. Nephrol. *25*, 687–697.
8. Albuquerque, E.X., Pereira, E.F., Alkondon, M., and Rogers, S.W. (2009). Mammalian nicotinic acetylcholine receptors: from structure to function. Physiol. Rev. *89*, 73–120.
9. Beckel, J.M., Kanai, A., Lee, S.J., de Groat, W.C., and Birder, L.A. (2006). Expression of functional nicotinic acetylcholine receptors in rat urinary bladder epithelial cells. Am. J. Physiol. Renal Physiol. *290*, F103–F110.
10. Xu, W., Gelber, S., Orr-Urtreger, A., Armstrong, D., Lewis, R.A., Ou, C.N., Patrick, J., Role, L., De Biasi, M., and Beaudet, A.L. (1999). Megacystis, mydriasis, and ion channel defect in mice lacking the alpha3 neuronal nicotinic acetylcholine receptor. Proc. Natl. Acad. Sci. USA *96*, 5746–5751.
11. Fowler, C.J., Griffiths, D., and de Groat, W.C. (2008). The neural control of micturition. Nat. Rev. Neurosci. *9*, 453–466.
12. Weber, S., Thiele, H., Mir, S., Toliat, M.R., Sozeri, B., Reutter, H., Draaken, M., Ludwig, M., Altmüller, J., Frommolt, P., et al. (2011). Muscarinic Acetylcholine Receptor M3 Mutation Causes Urinary Bladder Disease and a Prune-Belly-like Syndrome. Am. J. Hum. Genet. *89*, 668–674.
13. Braun, D.A., Lovric, S., Schapiro, D., Schneider, R., Marquez, J., Asif, M., Hussain, M.S., Daga, A., Widmeier, E., Rao, J., et al. (2018). Mutations in multiple components of the nuclear pore complex cause nephrotic syndrome. J. Clin. Invest. *128*, 4313–4328.
14. Hildebrandt, F., Heeringa, S.F., Rüschendorf, F., Attanasio, M., Nürnberg, G., Becker, C., Seelow, D., Huebner, N., Chernin, G., Vlangos, C.N., et al. (2009). A systematic approach to mapping recessive disease genes in individuals from outbred populations. PLoS Genet. *5*, e1000353.
15. MacArthur, D.G., Manolio, T.A., Dimmock, D.P., Rehm, H.L., Shendure, J., Abecasis, G.R., Adams, D.R., Altman, R.B., Antonarakis, S.E., Ashley, E.A., et al. (2014). Guidelines for investigating causality of sequence variants in human disease. Nature *508*, 469–476.
16. Sobreira, N., Schiettecatte, F., Boehm, C., Valle, D., and Hamosh, A. (2015). New tools for Mendelian disease gene identification: PhenoDB variant analysis module; and GeneMatcher, a web-based tool for linking investigators with an interest in the same gene. Hum. Mutat. *36*, 425–431.
17. Sobreira, N., Schiettecatte, F., Valle, D., and Hamosh, A. (2015). GeneMatcher: a matching tool for connecting investigators with an interest in the same gene. Hum. Mutat. *36*, 928–930.
18. Skok, V.I. (2002). Nicotinic acetylcholine receptors in autonomic ganglia. Auton. Neurosci. *97*, 1–11.
19. Chevalier, R.L., Forbes, M.S., and Thornhill, B.A. (2009). Ureteral obstruction as a model of renal interstitial fibrosis and obstructive nephropathy. Kidney Int. *75*, 1145–1152.
20. Becknell, B., Carpenter, A.R., Allen, J.L., Wilhide, M.E., Ingraham, S.E., Hains, D.S., and McHugh, K.M. (2013). Molecular basis of renal adaptation in a murine model of congenital obstructive nephropathy. PLoS ONE *8*, e72762.
21. Vernino, S., Sandroni, P., Singer, W., and Low, P.A. (2008). Invited Article: Autonomic ganglia: target and novel therapeutic tool. Neurology *70*, 1926–1932.
22. Vernino, S., Low, P.A., Fealey, R.D., Stewart, J.D., Farrugia, G., and Lennon, V.A. (2000). Autoantibodies to ganglionic acetylcholine receptors in autoimmune autonomic neuropathies. N. Engl. J. Med. *343*, 847–855.
23. Vivante, A., and Hildebrandt, F. (2016). Exploring the genetic basis of early-onset chronic kidney disease. Nat. Rev. Nephrol. *12*, 133–146.
24. Wangler, M.F., Gonzaga-Jauregui, C., Gambin, T., Penney, S., Moss, T., Chopra, A., Probst, F.J., Xia, F., Yang, Y., Werlin, S., et al.; Baylor-Hopkins Center for Mendelian Genomics (2014). Heterozygous de novo and inherited mutations in the smooth muscle actin (ACTG2) gene underlie megacystis-microcolon-intestinal hypoperistalsis syndrome. PLoS Genet. *10*, e1004258.
25. Milewicz, D.M., Østergaard, J.R., Ala-Kokko, L.M., Khan, N., Grange, D.K., Mendoza-Londono, R., Bradley, T.J., Olney, A.H., Adès, L., Maher, J.F., et al. (2010). De novo ACTA2 mutation causes a novel syndrome of multisystemic smooth muscle dysfunction. Am. J. Med. Genet. A. *152A*, 2437–2443.
26. Daly, S.B., Urquhart, J.E., Hilton, E., McKenzie, E.A., Kammerer, R.A., Lewis, M., Kerr, B., Stuart, H., Donnai, D., Long, D.A., et al. (2010). Mutations in HPSE2 cause urofacial syndrome. Am. J. Hum. Genet. *86*, 963–969.
27. Stuart, H.M., Roberts, N.A., Burgu, B., Daly, S.B., Urquhart, J.E., Bhaskar, S., Dickerson, J.E., Mermerkaya, M., Silay, M.S., Lewis, M.A., et al. (2013). LRIG2 mutations cause urofacial syndrome. Am. J. Hum. Genet. *92*, 259–264.
28. Roberts, N.A., Hilton, E.N., Lopes, F.M., Singh, S., Randles, M.J., Gardiner, N.J., Chopra, K., Coletta, R., Bajwa, Z., Hall,

R.J., et al. (2019). Lrig2 and Hpse2, mutated in urofacial syndrome, pattern nerves in the urinary bladder. Kidney Int. *95*, 1138–1152.

29. Halim, D., Brosens, E., Muller, F., Wangler, M.F., Beaudet, A.L., Lupski, J.R., Akdemir, Z.H.C., Doukas, M., Stoop, H.J., de Graaf, B.M., et al. (2017). Loss-of-Function Variants in MYLK Cause Recessive Megacystis Microcolon Intestinal Hypoperistalsis Syndrome. Am. J. Hum. Genet. *101*, 123–129.
30. Gauthier, J., Ouled Amar Bencheikh, B., Hamdan, F.F., Harrison, S.M., Baker, L.A., Couture, F., Thiffault, I., Ouazzani, R., Samuels, M.E., Mitchell, G.A., et al. (2015). A homozygous loss-of-function variant in MYH11 in a case with megacystis-microcolon-intestinal hypoperistalsis syndrome. Eur. J. Hum. Genet. *23*, 1266–1268.
31. Chevalier, R.L. (2015). Congenital urinary tract obstruction: the long view. Adv. Chronic Kidney Dis. *22*, 312–319.

3. Danksagung

Ich bedanke mich herzlich bei meinem Doktorvater Prof. Dr. med. Heiko Reutter und den Mitarbeitern unserer Arbeitsgruppe, darunter besonders Prof. Dr. rer. nat. Michael Ludwig, Dr. rer. nat. Rong Zhang und Pia Uerdingen für die hervorragende Betreuung, die beständige Unterstützung und die schöne Zeit im Labor. Der BONFOR-Forschungskommission, dem Deutschen Akademischen Austauschdienst (DAAD) und dem Biomedical Exchange Program (BMEP) danke ich für die finanzielle Förderung der Forschungsvorhaben. Prof. Dr. med. Friedhelm Hildebrandt und seiner Arbeitsgruppe danke ich für die ausgezeichnete Betreuung im Labor und für die sehr schöne und interessante Zeit in Boston. Außerdem bedanke ich mich bei allen Patientinnen und Patienten, die an unseren Studien teilgenommen haben. Bei meinem Mann, meinen Eltern und Schwestern bedanke ich mich für ihre stetige Unterstützung.